HEAT CAPACITY OF N-PENTANE LIQUID AT ELEVATED PRESSURES

Ding-yu Peng

Leonard I. Stiel Dissertation Supervisor

ABSTRACT

Experimental heat capacity data have been obtained for n-pentane in the liquid region for temperatures from 140° to 300°F and pressures between 400 and 3,000 psia by using a flow calorimeter system. The apparatus consisted of a calorimeter and constant temperature bath through which the fluid is circulated at a steady rate. The volumetric flow rate is measured with a turbine flowmeter and digital counter. The electrical energy to the main calorimeter heater is applied by a D.C. power supply. The heat capacity of the fluid is calculated from the fluid temperature rise, the mass flow rate, and the energy input.

The heat capacity data for n-pentane are estimated to be accurate to within 1%. The experimental values have been compared with those resulting from density and enthalpy data for the substance and those calculated from generalized

correlations for the heat capacity departure of non-polar fluids. The experimental data agree most closely with the values derived from the experimental density data (maximum deviation of approximately 3%), and are consistent with experimental data for the heat capacity of the saturated liquid.

The generalized correlation presented by Edmister for the prediction of heat capacity values of normal fluid has been tested with experimental data for methane, nitrogen, propane, and n-pentane. The predicted values do not show good agreement with experimental results. More reliable prediction method is to be developed.

HEAT CAPACITY OF N-PENTANE LIQUID AT ELEVATED PRESSURES

A Dissertation

Presented to

the Faculty of the Graduate School

University of Missouri

In Partial Fulfillment

of the Requirements for the Degree

Doctor of Philosophy

---

by

Ding-yu Peng

December 1972

Leonard I. Stiel Dissertation Supervisor

ACKNOWLEDGEMENTS

The author wishes to express his sincere gratitude to Dr. Leonard I. Stiel for his patience, guidance, and encouragement throughout this study.

The author is grateful to the donors of the Petroleum Research Fund, administered by the American Chemical Society, for the support of this work.

The author wishes to thank Dr. George W. Preckshot for his many assistances in eradication of the experimental difficulties. Thanks are also due to Dr. Richard M. Angus and Dr. Richard C. Warder for reading the manuscript. The partial financial support provided by the Engineering Experiment Station is gratefully acknowledged. Appreciation is also extended to the Research Council of the Graduate School for their support of purchasing a high pressure turbine pump.

Finally, the author is especially indebted to his wife, Ping-Ji, for her encouragement, understanding, and the burden she shared during this work.

TABLE OF CONTENTS

CHAPTER PAGE

LIST OF TABLES

LIST OF FIGURES

FIGURE PAGE

CHAPTER I

INTRODUCTION

The heat capacity of fluids is one of the most important thermodynamic properties as evidenced by its being so frequently used in engineering calculations and studies of thermodynamic and transport properties. Nevertheless, the determination of liquid heat capacities at temperatures above the normal boiling point has received very little attention. Not only that there are only sparse experimental data in this region, but also that the existing correlation methods for predicting the heat capacity of liquids at elevated pressures and temperatures need detailed comparisons with experimental data.

Therefore, in this study a flow calorimeter system has been constructed with a view to measure the isobaric heat capacity of polar and non-polar fluids at their liquid and dense gaseous regions. The experimental data obtained will be used to check the reliability of existing methods for prediction of heat capacity of fluids and, when sufficient data have been gathered, to establish more reliable correlation techniques for the calculation of the heat capacity values. Because there are extensive thermodynamic and volumetric data available for n-pentane, and there are no experimental heat capacity data for this fluid, it is therefore chosen as the initial substance for this investigation.

CHAPTER II

LITERATURE SURVEY

A. Experimental Methods

The experimental determination of the isobaric heat capacity of fluids can be dated back to the late 18th century when Crawford (15) attempted to measure the relative heat capacities of gases to water by immersing a heated flask which contained gases into cold water and noting the temperature rise of the water. In 1924 Partington and Shilling published the book entitled "Specific Heats of Gases" (48). A detailed description of each worker's method and apparatus as well as tabulation of their results was presented. Masi (40) presented a survey of all literature reports of experimental determination of heat capacities of gases for the period 1925 to 1952. Yesavage et al (78) supplemented earlier work by Faulkner (20) and Barieau (3) in an effort to describe the various experimental methods for the determination of heat capacities of fluids.

There are two categories of experimental methods for the determination of the heat capacities of fluids, namely, direct methods and indirect methods. In the indirect methods, heat capacity values are obtained either from other measured physical properties through an equation of state, or by compar-

ison with a calibrating fluid having a known heat capacity and/or known latent heat. The indirect methods utilized include the isentropic expansion method (7, 8, 28), sonic velocity method (14, 23, 47, 65, 66), resonance method (13), self-sustained oscillations method (29), flow comparison method (5), and P-V-T method (18). In the direct methods, heat capacity values are obtained with the employment of calorimeters. A measured amount of energy, Q, in the form of heat is added to or withdrawn from the fluid having mass m which is enclosed in the calorimeter. The resulting temperature change of the fluid, ΔT, is noted. The heat capacity of the fluid is calculated by the simple expression

$$C = \frac{Q}{m \Delta T} \qquad (1)$$

where C is the heat capacity of the fluid. Corrections have to be made due to imperfections of the calorimeter. Recently a description of various kinds of calorimeters was given by Ginnings (21).

Basically the direct methods involve two different types of calorimeters: non-flow calorimeters and flow calorimeters. The former are usually called constant volume calorimeters and are used to measure the heat capacity at constant volume. Michels and Strijland (43), DeNevers and Martin (17), and Voronel' and Strelkiv (73) were among the workers who used this kind of calorimeter. Flow calorimeters can be designed

in a number of ways to suit the different operation modes which lead to the data of interest. Besides their being used to measure the isobaric heat capacity, flow calorimeters have been used to measure Joule-Thomson coefficient (25, 27, 49, 57), the isothermal throttling coefficient (26, 41), the enthalpy of pure fluids (12, 24, 32, 33, 34, 35, 39, 76, 78, 80), and the enthalpy of mixtures (33, 34, 35, 79).

B. Flow Calorimeters

Callendar and Barnes (11) used a continuous flow electric calorimeter to determine the isobaric heat capacity of water. In this calorimeter, fluid at constant flow rate passed through an electrically heated tube with a temperature measuring device located at both the inlet and outlet of the tube. By measuring the electric energy input, the mass flow rate, and the temperature rise, the apparent heat capacity of the fluid was obtained. The true heat capacity of the fluid was obtained by making corrections for the heat leak from the calorimeter.

Since then quite a few flow calorimeters have been developed for the determination of the isobaric heat capacity. Partington and Shilling (48) reviewed and described in detail several of the early designs. Callendar (10) enumerated the following advantages for the use of a flow calorimeter: "(I) since the temperature of each part of the apparatus is steady

under steady flow conditions, no correction for the heat capacity of the apparatus is required; (II) the size of the apparatus can be relatively small, thereby maintaining a small heat loss and providing a quick response to a change of conditions; (III) flow of the fluid itself supplies agitation, elimination a stirring device; and (IV) heat loss can be reduced by jacketing each part of the apparatus with its own flow."

Osborne, Stimson, and Sligh (44) built a refined flow calorimeter capable of measuring heat capacity of gases at pressures up to 100 atmospheres and temperatures to 150°C. Their calorimeter system has the outstanding characteristics of having a size appropriate for a moderately small quantity of test fluid, negligible thermal leak, and precisely controlled constant flow rate. Results having an accuracy of better than 0.1% were obtained with this calorimeter (45).

Krase and Mackey (30, 31, 38) used a different electric-heating method to measure the heat capacity of nitrogen at pressures up to 700 atmospheres and temperatures to 150°C. Nitrogen gas was passed through a coil of steel tubing embedded in an electrically heated copper casting. The electric heat was to keep the copper casting at isothermal conditions while the nitrogen gas took away heat from it. The heat capacity of nitrogen was obtained by measuring the electrical power supplied to the casting, the gas temperature rise, and

gas flow rate. Corrections were made for heat loss due to conduction and heat gain from electrical induction.

Pitzer (50) initiated the design of a non-adiabatic type of flow calorimeter. For this kind of flow calorimeter the fractional heat loss of the calorimeter proper is inversely proportional to the flow rate of the test fluid. Improvements in this type of calorimeters have been discussed by workers at U. S. Bureau of Mines (42, 74). However, most of these calorimeters are designed for low pressure operations.

At high pressures, especially at conditions when high temperature is also called for, metering, circulation, and regulating of the test fluid are only part of the major difficulties in flow calorimetry. Other difficulties involve the sealing of the electric heating element in the pressurized chamber, measuring the true temperatures which represent the states of the flowing fluid, and minimizing the heat leak.

Schrock (64) built a flow calorimeter to measure the isobaric heat capacity of carbon dioxide over the range of pressures and temperatures from ambient conditions to 1,000 psig and 1,000°F in an open cycle. The use of a heat exchanger to cool the hot gas leaving the calorimeter enabled the measurement of the gas flow rate with a volumetric meter. Radiation shields as well as guard heaters were used to eliminate the heat loss from the calorimeter which is enclosed in an evacuated casing. Accuracy of the results were estimated to

be within 0.5%.

The flow calorimeter system built by workers at the University of Michigan (20, 24, 39, 79, 80) is a closed-flow system capable of measuring heat capacity of gases or gaseous mixtures at temperatures from -280° to 300°F and pressures from 100 to 2,000 psia. Mass flow rate was calculated using an empirical equation for the volumetric flow rate determined with a linear flowmeter. Buffer tanks were employed to ensure essentially constant flow rate. Heat leak of the calorimeter was reduced using devices similar to that used in Schrock's experiments. Accuracy of the heat capacity measurements was about 1%.

Experimentalists in Russia have also been interested in flow calorimetry. Sirota and coworkers at All-Union Heat Engineering Institute (67, 68, 69, 70, 71) developed a closed-loop flow calorimeter system for measuring heat capacity of water and steam at pressures from 20 to 1,000 kg/cm^2 and temperatures from -10° to 700°C. Circulation of the high pressure water was provided by a gear pump which was immersed in the compressed water. The calorimeter proper was located in a thermostatted bath and consisted of a double-coiled tubing. Water first flowed through the outer spiral tubing then through the inner spiral tubing where the fluid took up heat supplied by the main heater which was located at the center of the inner coil. Heat loss was reduced to a minimal amount with this

design. Temperature measuring elements were located at the inlet of the outer spiral tubing and the outlet of the inner tubing respectively. A specially designed calorimeter-flowmeter was used in their experiment to measure the mass flow rate of water. The fact that the isobaric heat capacities of water at ambient temperatures are known with a high degree of accuracy and are affected little by pressure made the flow rate measurement by calorimetric means possible.

Rivkin and Gukov (56) built a closed circulation flow calorimeter system to investigate the isobaric heat capacity of carbon dioxide at pressures up to 250 kg/cm^2 in the temperature range 10° to $130^{\circ}C$. This system was similar to Sirota's except that the calorimeter-flowmeter was operated at a mean temperature of about $300^{\circ}C$ to measure the mass flow rate of carbon dioxide. Data reported has a maximum error of 1 to 2 %. Other flow calorimeters include those built by Altunin and Kuznetsov (1) and by Sheindlin and coworkers (63).

C. Thermodynamic Data for n-Pentane

Young and coworkers (58, 81) determined the pressure-volume-temperature relation of n-pentane from 104° to $536^{\circ}F$ at pressures up to 10,000 psia. Young (81) and Timmermans(72) studied the density of the saturated liquid at much lower temperatures. Sage and coworkers (61, 62) investigated the volumetric behavior of this hydrocarbon at temperatures

between 70° and 460°F and pressures up to 10,000 psia and calculated enthalpy-pressure coefficients and isothermal enthalpy changes from the volumetric data and other information. Beattie, Levine, and Douslin (4) measured the compressibility of n-pentane from 200°to 300°C and from a density of 1 to 7 moles per liter and determined constants of the Beattie-Bridgeman equation of state to represent the data. Li and Canjar (36) determined the pressure-volume-temperature relationships of n-pentane over a temperature range from 212° to 572°F for pressures up to 3,200 psia and found that their results to be in good agreement with those of the other investigators. Brydon, Walen, and Canjar (9) used the experimental volumetric data of Sage and Lacey (61), of Beattie, Levine, and Douslin (4), and of Li and Canjar (36) to evaluate thermodynamic properties of n-pentane by numerical methods over a range of 100° to 570°F in temperature and 10 to 3,000 psia in pressure. Brydon, Walen, and Canjar (9) fitted the volumetric data in the liquid phase by the equation

$$v = (\mu_o + \mu T) + (\eta_o + \eta T)P + (\rho_o + \rho T)P^2 + r_v \qquad (2)$$

where μ's, η's, and ρ's are constants and r_v is the residual volume necessary to have the equation fit the data exactly, and calculated enthalpy values from 100° to 380°F at six pressures between 500 and 3,000 psia.

Lenoir, Robinson, and Hipkin (32) measured the enthalpy

of n-pentane from 100° to 700°F with pressures up to 1,400 psia. Pattee and Brown (49) measured the Joule-Thomson coefficient of the gas for temperatures from 200° to 900°F at pressures up to 10,000 psia. Pitzer (50, 51) and Pitzer and Kilpatrick (52) measured the heat capacity of the gas at atmospheric pressure for temperatures from 298° to 1,500°K. Sage and coworkers (60) measured the constant volume heat capacity of this fluid in the two phase region and used volumetric data to calculate the heat capacity of the saturated liquid. American Petroleum Institute Research Project 44 (59) listed the ideal gas heat capacity for n-pentane in the temperature range -200° to 2,200°F.

D. Methods for Prediction of the Isobaric Heat Capacity

Lydersen, Greenkorn, and Hougen (37) have used the critical compressibility factor z_c as a third parameter in addition to T_R and P_R to develop generalized correlations for several thermodynamic properties. Lydersen, Greenkorn, and Hougen (37) differentiated their tables for the reduced enthalpy departure $(\tilde{H}-\tilde{H}^o)/T_c$ with respect to reduced temperature at constant reduced pressures to develop a correlation for the departure of the heat capacity from the ideal gas heat capacity, $\tilde{C}_p-\tilde{C}_p^o$, only for $z_c=0.27$. Lydersen et al (37) did not prepare tables of $\tilde{C}_p-\tilde{C}_p^o$ values for other values of z_c because they felt that

the inherent inaccuracy in the double graphical differentiation of compressibility factor data did not warrant the inclusion of the effects of a third parameter for this property. Weiss and Joffe (75) used values of $\tilde{C}_p - \tilde{C}_p^o$ obtained analytically from the Benedict-Webb-Rubin equation of state for methane, ethane, ethylene, propane, and normal butane to produce a plot of $\tilde{C}_p - \tilde{C}_p^o$ as a function of T_R and P_R for reduced pressures from 0.2 to 15 and reduced temperatures from 1.0 to 5.5. Weiss and Joffe (75) found that substantial differences exist between their correlation for $\tilde{C}_p - \tilde{C}_p^o$ and that of Lydersen, Greenkorn, and Hougen.

Curl and Pitzer (16) expressed the dimensionless effect of pressure on enthalpy $(\tilde{H}^o - \tilde{H})/RT_c$ as functions of T_R, P_R, and ω by the equation

$$\frac{\tilde{H}^o - \tilde{H}}{RT_c} = \left(\frac{\tilde{H}^o - \tilde{H}}{RT_c}\right)^{(o)} + \omega \left(\frac{\tilde{H}^o - \tilde{H}}{RT_c}\right)^{(1)} \qquad (3)$$

where $\left(\frac{\tilde{H}^o - \tilde{H}}{RT_c}\right)^{(o)}$ and $\left(\frac{\tilde{H}^o - \tilde{H}}{RT_c}\right)^{(1)}$ are functions of T_R and P_R, and ω is the acentric factor defined by Pitzer and coworkers (53) as

$$\omega = -\log P_R - 1.0 \qquad (4)$$

with P_R the reduced vapor pressure at $T_R = 0.7$.

Edmister (19) expressed the heat capacity departure as

$$\tilde{C}_p - \tilde{C}_p^o = (\tilde{C}_p - \tilde{C}_p^o)^{(o)} + \omega \ (\tilde{C}_p - \tilde{C}_p^o)^{(1)} \qquad (5)$$

and developed plots of $(\tilde{C}_p - \tilde{C}_p^o)^{(o)}$ and $(\tilde{C}_p - \tilde{C}_p^o)^{(1)}$ as functions of reduced temperature and reduced pressure by the use of the

functions for the derivative compressibility factor z_T presented by Reid and Valbert (54), through the relationship

$$\tilde{C}_p - \tilde{C}_p^o = -R\int_0^{P_R} \frac{T_R}{P_R}\left(\frac{\partial z_T}{\partial T_R}\right)_{P_R} d\,P_R \qquad (6)$$

where $$z_T = z + T_R\left(\frac{\partial z}{\partial T_R}\right)_{P_R} = z_T^{(0)} + \omega\ z_T^{(1)} \qquad (7)$$

Edmister also obtained values for $(\tilde{C}_p - \tilde{C}_p^o)^{(0)}$ and $(\tilde{C}_p - \tilde{C}_p^o)^{(1)}$ by differentiating the functions for the dimensionless effect of pressure on enthalpy presented by Curl and Pitzer (16). Similar results were obtained by the two methods. API Technical Data Book (2) presented both tables and graphs of $\left(\frac{\tilde{C}_p^o - \tilde{C}_p}{R}\right)^{(0)}$ and $\left(\frac{\tilde{C}_p^o - \tilde{C}_p}{R}\right)^{(1)}$ for the gas region only.

Yen and Alexander (77) have used experimental and derived enthalpy data for 28 non-polar and polar substances to improve and extend the correlation of Lydersen, Greenkorn, and Hougen (37) for the reduced enthalpy departure. Both graphs and analytical expressions were presented for values of the critical compressibility factor of 0.23, 0.25, 0.27, and 0.29. These analytical expressions are differentiable to produce functions for the heat capacity departure. However, they are yet to be tested with experimental data.

For normal liquids, Yuan and Stiel (83) expressed the saturated liquid heat capacity departure, $\tilde{C}_\sigma - \tilde{C}_p^o$, as

$$\tilde{C}_\sigma - \tilde{C}_p^o = (\tilde{C}_\sigma - \tilde{C}_p^o)^{(0)} + \omega\ (\tilde{C}_\sigma - \tilde{C}_p^o)^{(1)} \qquad (8)$$

Yuan and Stiel (83) obtained the coefficients of Equation 8 by correlating the experimental heat capacity data for 21 normal liquids for reduced temperatures between T_R=0.4 and T_R=0.96. For polar fluids, Yuan and Stiel (83) expressed the saturated liquid heat capacity departure, $\Delta\tilde{C}_\sigma$ as

$$\Delta\tilde{C}_\sigma = \Delta C_\sigma^{(0)} + \omega \Delta C_\sigma^{(1)} + x\Delta C_\sigma^{(2)} + x^2\Delta C_\sigma^{(3)} + \omega^2\Delta C_\sigma^{(4)} + \omega x \Delta C_\sigma^{(5)} \quad (9)$$

where x is a parameter defined by Halm and Stiel (22) as

$$x = \log P_R|_{T_R=0.6} + 1.70\omega + 1.552 \quad (10)$$

Yuan and Stiel (83) obtained the coefficients of Equation 9 by correlating the experimental heat capacity data for 21 normal fluids and for 16 polar liquids for reduced temperatures between T_R=0.44 and T_R=0.94.

Other generalized methods for the estimation of heat capacity of liquids were discussed by Reid and Sherwood (55), Bondi (6), and Yuan (82).

CHAPTER III

EXPERIMENTAL APPARATUS

A schematic diagram of the experimental system is shown in Figure 1. The apparatus consists primarily of a flow calorimeter and a constant temperature bath through which the test fluid flows at a steady rate. A pressure generator is used to maintain the supply of high pressure fluid in the high pressure vessel. From this high pressure vessel, the test fluid is circulated at constant flow rate by means of the turbine pump through a helical coil of stainless steel tubing immersed in the constant temperature bath. The test fluid exchanges heat with the bath so that at the inlet of the calorimeter the test fluid maintains a constant temperature. The fluid temperatures are measured at both the inlet and the outlet of the calorimeter proper by means of thermopiles. An electric heater is installed around the inner part of the calorimeter to heat the test fluid. Pressure transducers are mounted at the ends of the calorimeter for accurate measurement of the fluid pressure. A volumetric flowmeter is located downstream of the calorimeter for the purpose of measuring the flow rate of the test fluid. Then the test fluid returns to the high pressure vessel to form a closed-loop for the flow calorimeter system. Details of the components of the experimental apparatus are described as follows:

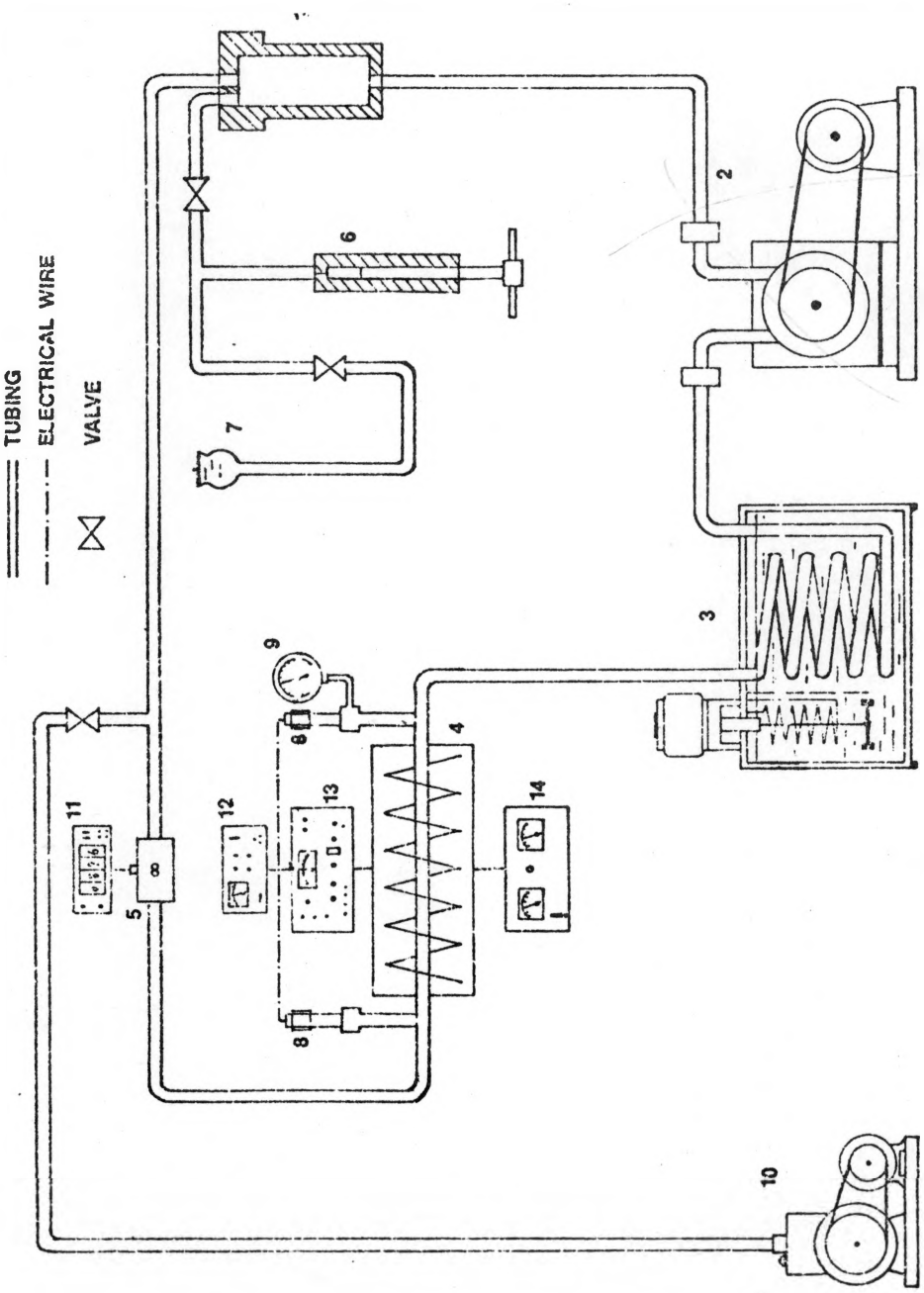

Figure 1. Schematic diagram of apparatus

Key to Figure 1

1. Pressure Vessel
2. High Pressure Turbine Pump
3. Constant Temperature Bath
4. Calorimeter
5. Turbine Flowmeter
6. Pressure Generator
7. Charging Assembly
8. Pressure Transducers
9. Pressure Gauge
10. Vacuum Pump
11. Frequency Counter
12. Low Voltage D.C. Power Supply
13. Differential Potentiometer
14. D. C. Power Supply

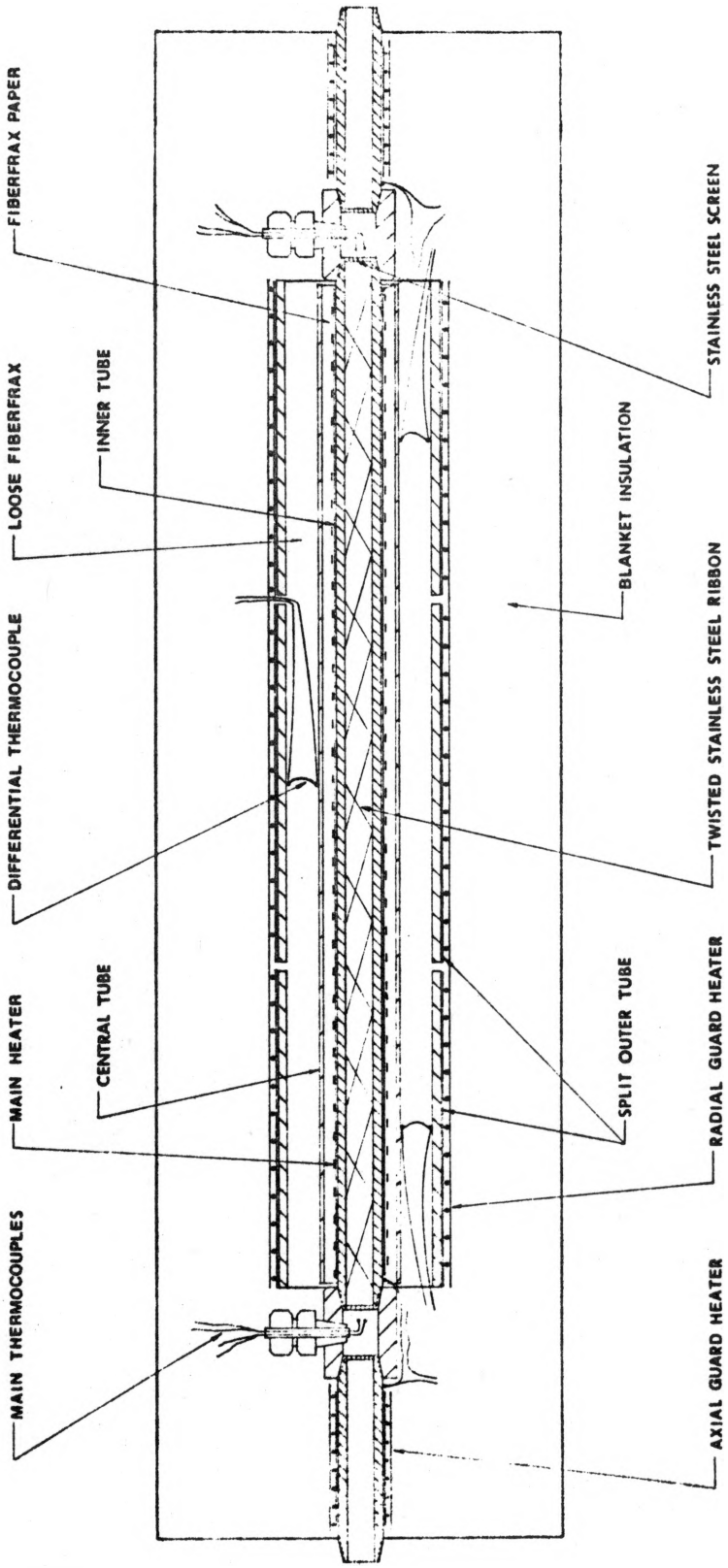

Figure 2. Flow calorimeter

A. Calorimeter

A diagram of the flow calorimeter is presented in Figure 2. The calorimeter (custom built by Thermo-Physics Company) is about six feet long and five inches in diameter. It consists of a test section, which is approximately four feet long, and two end-guards, which are connected to the test section using fittings. The test section consists of three concentric tubes having dimensions of 0.500" O.D. x 0.260" I.D., 0.875" O.D. x 0.745" I.D., and 1.750" O.D. x 1.500" I.D., respectively. All tubes were made of type 304 stainless steel. At each end of the inner tube a chromel-alumel thermocouple was welded to the surface. Nichrome ribbon having resistance of 0.93 ohms per foot was uniformly wrapped around the inner tube at four and one-half turns per inch after the tube had been insulated with a layer of 0.031 inches thick asbestos paper. The total resistance of this heating element which served as the main heater of the calorimeter was about 27 ohms at room temperature. Stainless steel screens were silver soldered to the inlet and outlet of the inner tube to enhance turbulent behavior and hence insure good mixing of the test fluid. Twisted stainless steel ribbon was also installed inside the inner tube to promote the heat transfer rate.

Three differential thermocouples made of chromel-alumel were attached to the outside surface of the central tube and

the inside surface of the outer tube. The outer tube was divided into three sections. Each section was wrapped with chromel wire serving as a guard heater to minimize radial heat conduction losses of the calorimeter. The end-guard heaters were also provided with chromel-alumel differential thermocouples and were wrapped with chromel heating wire. The purpose of the end-guard heaters was to minimize axial heat conduction losses in the test section. Two A.W.G.#20 copper-constantan thermopiles, one each at the inlet and the outlet of the test section, were used to measure the fluid temperatures. Each thermopile consists of two thermocouple junctions and was installed in its place using Conax MTG-20-A4 thermocouple fittings with lava seal. The wiring of the thermopile is shown in Figure 3.

Each guard heater was independently controlled using one of five variable autotransformers (Model 10-B, Powerstat). Regulated manually, each autotransformer could deliver a maximum output of 300 watts at 132 volts. The calorimeter main heater was connected to a regulated D.C. power supply (Model L-136-9, Deltron) which can deliver a maximum current of 9 amperes in the adjustable voltage range of 128 to 144 volts. Voltage taps of the main heater were connected to a differential potentiometer (Model 7564, Leeds and Northrup) for accurate measurement of the voltage drop across the main heater. The current in the main heater was accurately measured with

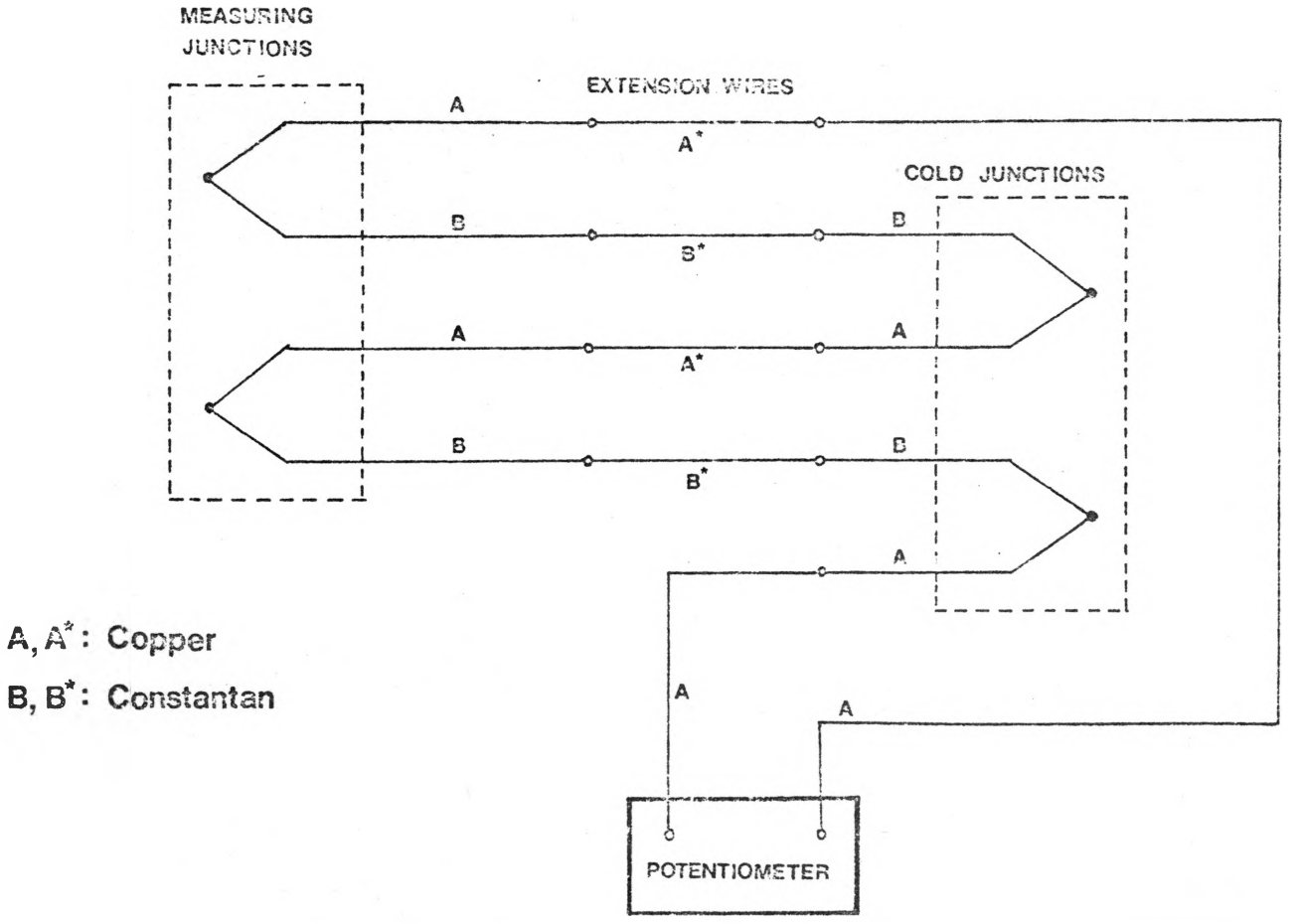

Figure 3. Circuit of main thermopile

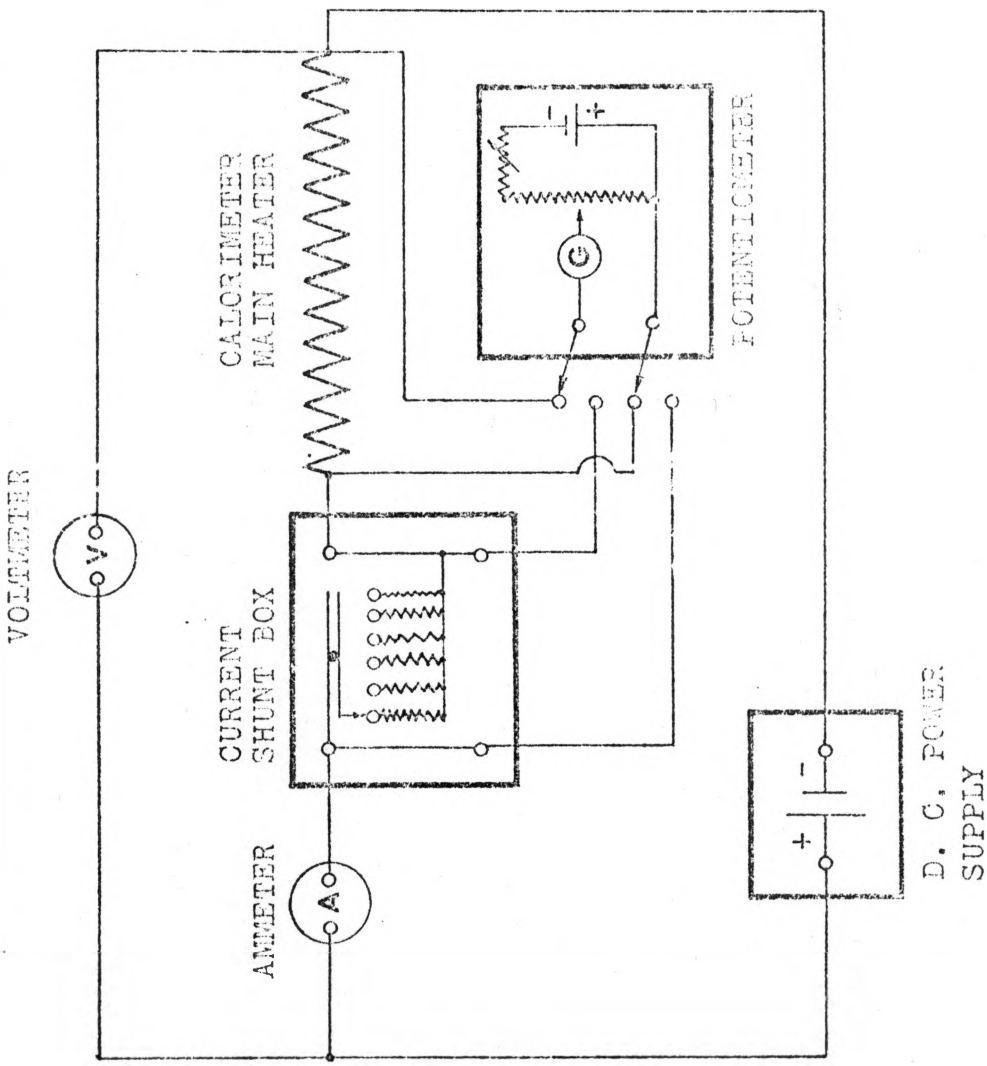

Figure 4. Circuit of main heater

the potentiometer in conjunction with a current shunt box (Model 4385, Leeds and Northrup). A diagram showing the wiring of the main heater is presented in Figure 4.

All thermocouple outputs were measured with the differential potentiometer using a rotary switch. The reference junctions for the thermocouples were immersed in a Dewar flask containing mixtures of distilled water and compacted, crushed ice made from distilled water.

B. High Pressure Turbine Pump

The high pressure turbine pump (custom built by Pressure Products Industries) is a unit for circulating the test fluid in the closed system. It can withstand a system pressure of 4,500 psig at 300°C. A 3/4 horsepower electric motor was used in conjunction with a variable gear box to drive the pump shaft.

The pump uses a packed stuffing box drive assembly to provide both seal and lubrication at high pressures as well as high temperatures. The stuffing box as shown in Figure 5 was packed with one set of Teflon asbestos rings, a lantern ring, and an "O" ring seal. Lubricant supplied by the intensifying cylinder entered the stuffing box and spread to the packings through the lantern ring. The Teflon asbestos rings and the "O" ring seal prevent the lubricant from leaking to the pump and to the atmosphere respectively. The drive shaft of the pump was guided by the bottom bearing and the packing back-up

so that it could rotate concentrically in the packing. The drive shaft was drilled for the length of the packing area and cooling water was able to circulate in it to reduce the operational and frictional heat. A floating hub shaft assembly permitted the shaft to adjust itself for any slight misalignment.

The intensifying cylinder which supplied lubricant to the stuffing box is shown in Figure 6. It was fitted with a piston which isolated the lubricant from the fluid being pumped. The piston rod extended out through the cover of the lubricant end of the cylinder not only served as an indication of the lubricant level but also reduced the effective area of the lubricant side of the piston. The intensifying action of differential areas of the intensifying cylinder thus forced the lubricant into the stuffing box at the lantern ring. The pressure within the system was released and lubricant was added manually to the cylinder after the removal of the top main nut and cover of the cylinder. The piston was then pushed to contact the bottom of the cylinder. Since no contamination of the test fluid is permitted in this study, the lubricant used is the same as the test fluid in the pump.

C. Flow Measurement System

The apparatus for measuring the flow rate of the test fluid consists of a volumetric turbine flowmeter and a frequency

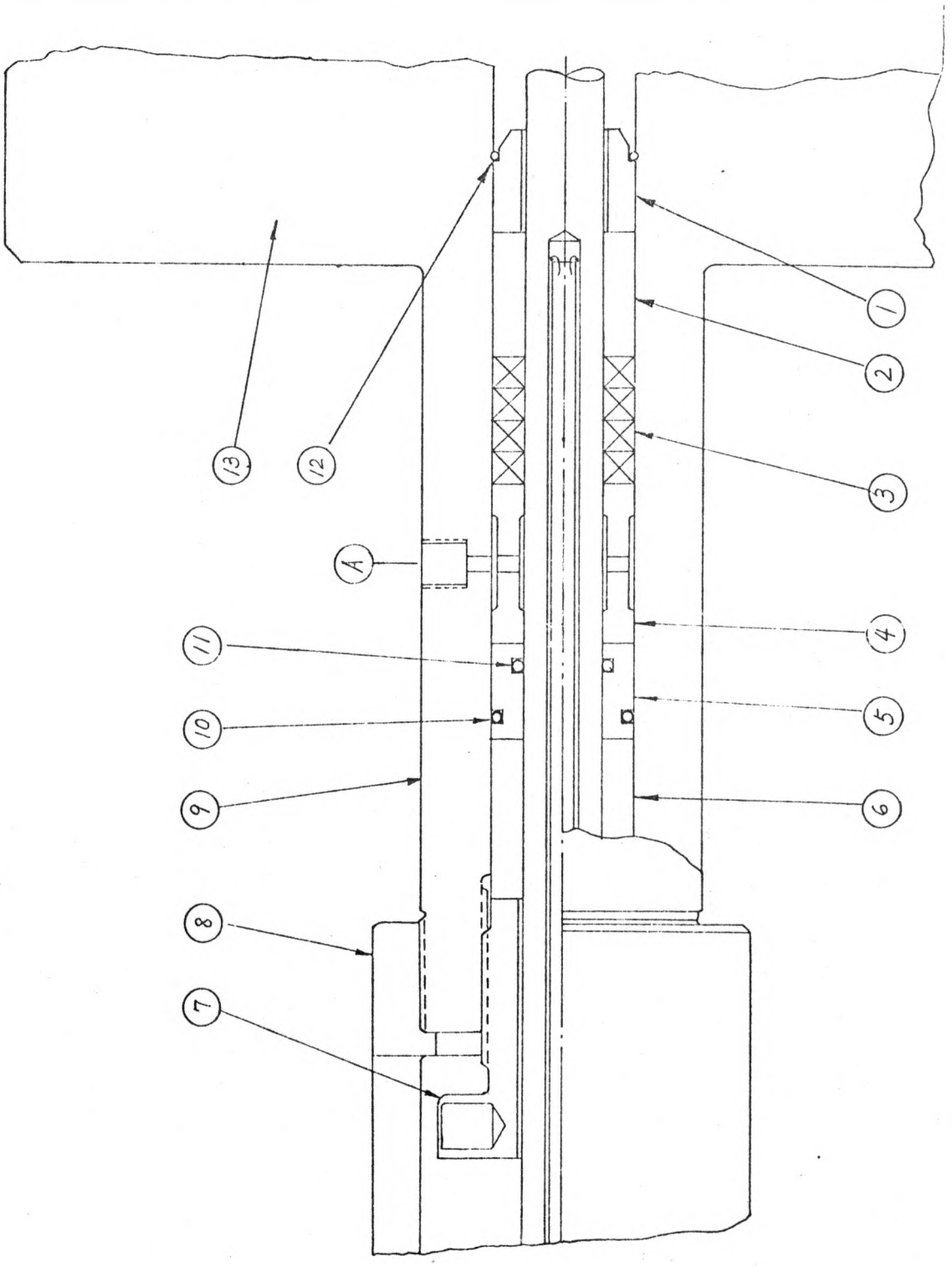

Figure 5. Stuffing box

Key to Figure 5

1. Bearing Support
2. Bottom Bearing
3. Teflon/Astestos Packing
4. Lantern Ring
5. "O" Ring Seal
6. Packing Back-up
7. Packing Gland Nut
8. Bearing Housing
9. Stuffing Box
10. "O" Ring
11. "O" Ring
12. Snap Ring
13. Pump Body
14. Drive Shaft

(A) Lubrication Port

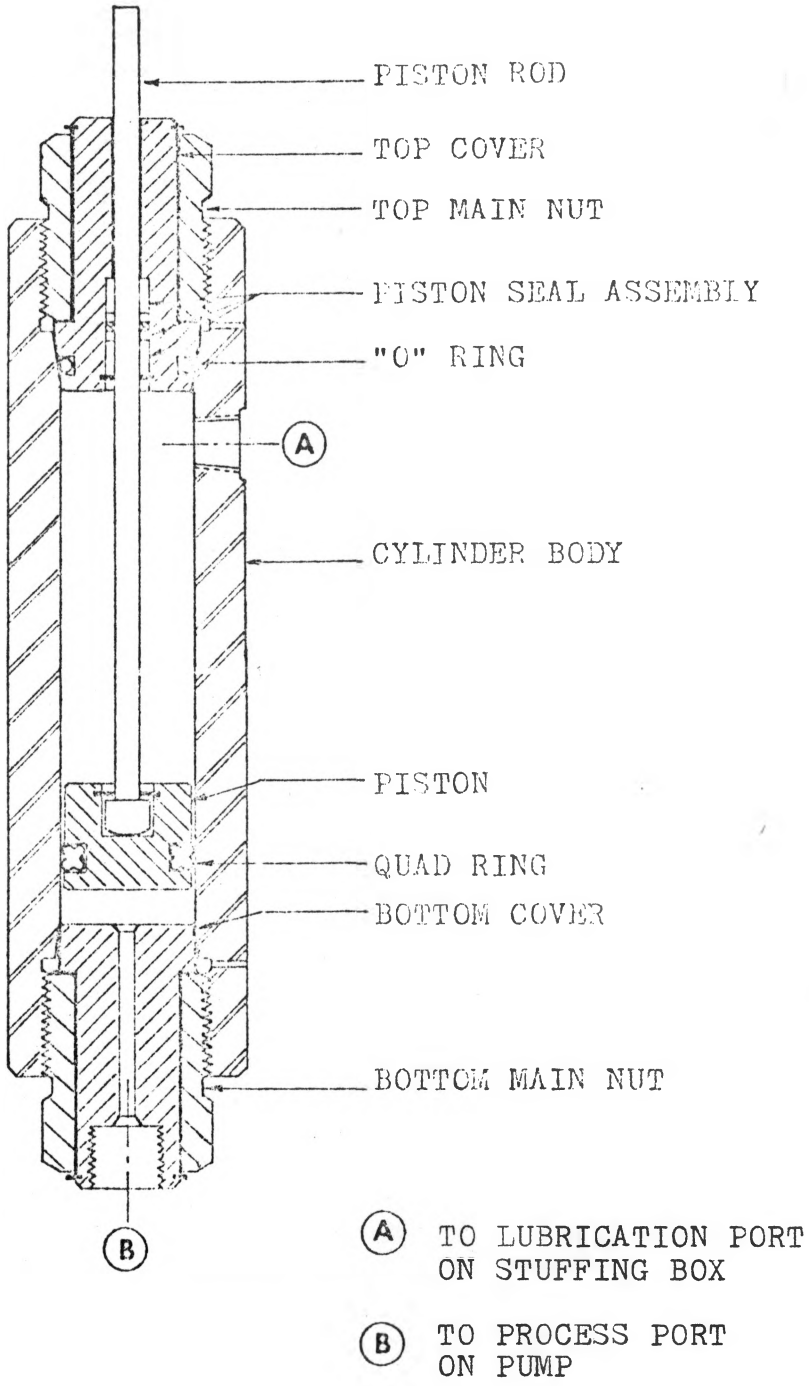

Figure 6. Intensifying cylinder

counter. The turbine flowmeter (Model FT-8M-2LB, Flow Technology Inc.) is essentially a velocity sensing device. It contains a freely-suspended, bladed rotor, positioned axially in line with the flowing fluid, which rotates at a speed directly proportional to the average velocity of the flowing fluid. The tips of the rotating blade pass through the field of an externally-mounted magnetic pick-off coil assembly and induce an alternating electric current with both frequency and amplitude proportional to rotational speed of the rotor. Since the flow passage area at the rotor is fixed, the frequency or amplitude of the alternating current represents the volumetric flow rate of hte fluid. The frequency of the output of the flowmeter ranges from 160 to 1,800 cycles per second over the usable range of 0.2 to 2.0 gallons per minute. The flowmeter has a pressure rating of 3,000 psia.

The output signal from the flowmeter is fed into the frequency counter (Model 5230K, Berkeley). This electronic counter is capable of measuring frequency from D.C. to 100 kHz. It contains an electronic gate and a chain of decimal counting units. When this counter is operated for frequency measurements two pulse sources are used. One of the input trigger channels in the counter converts the sinusoidal signal received from the flowmeter into sharp pulses. A time base generator in the counter produces similar pulses separated by a precise time interval. The decimal counting units then

determine and display the number of pulses provided by the input trigger channel over the known time interval between start and stop pulses from the time base generator.

D. Constant Temperature Bath

The fluid coming out from the discharge end of the turbine pump enters a coiled tubing immersed in a constant temperature bath (Model TEB-45-300HT, Neslab Instruments, Inc.). The coiled tubing was made of type 304 stainless steel high pressure tubing having dimensions of 9/16" O.D. x 5/16" I.D.. The coil was about 10 inches in diameter and had a heat transfer area of about 2 square feet.

The bath has a working space of 10" w x 17" l x 12" h and contains about 45 liters of bath fluid. Distilled water was used as bath fluid for the temperature range 130°to 210°F while silicone oil (SF-96-50, General Electric) was used for the temperature range 210° to 300°F. The temperature uniformity of the bath fluid was controlled to within 0.01°C by agitation with a pump. The bath uses a quartz heater and a solid state relay in conjunction with mercury thermo-regulator to achieve temperature control of better than ±0.005°C. In this study, for temperatures below 200°F, it was necessary to pass cooling water through a coil immersed in the bath to remove the excess heat as the test fluid entered the coiled tubing at a slightly higher temperature than that of the bath

fluid. The temperature of the test fluid at the inlet of the calorimeter was controlled to within 0.01°F by this bath at all times.

E. Pressure Measurement System

A Bourdon-tube gauge (Model WB-7-1, Astra) was employed in this study to indicate roughly the system pressure. This gauge was located at the upstream side of the calorimeter. It had a usable pressure range of 0 to 7,500 psig with 50 psi resolution. The pressure in the calorimeter was accurately determined by using two pressure transducers (Model GT-70-118, General Transducer Company). One transducer was located at the inlet of the calorimeter while the other was located at the outlet.

Each pressure transducer was virtually a balanced bonded strain gage forming four active arms of a Wheatstone-bridge circuit. The pressure applied to the sensing element of the transducer caused the resistance of the circuit to change and thus unbalanced the circuit. The resulting potential difference across the output terminals of the unbalanced circuit was therefore a measure of the magnitude of the applied pressure. The potential differences were measured with the Leeds and Northrup differential potentiometer. A low voltage D.C. power supply (Model IP-27, Heath Company) was used to provide the 10.000 VDC excitation voltage required for the transducers.

The transducers can be used from ambient temperature to 750°F with the provisions for water cooling. Calibration data furnished by the manufacturer shows that repeatabilities of better than ±2.5 psi can be obtained for the usable pressure range of 0 to 5,000 psig.

F. Pressure Generator

The pressure generator (Model 62-6-10, High Pressure Equipment Company) is basically a manually driven fluid injector. Its body was constructed from type 316 stainless steel and rated for a pressure of 10,000 psi. About 30 ml. of fluid can be injected into the high pressure system when its plunger makes a full stroke displacement. Figure 7 shows this unit and other necessary fittings. Valve 2 is closed at all times except when charging fluid into the high pressure vessel or releasing the pressure is necessary. To fill the pressure generator with test fluid, valve 2 remains closed while valve 1 is kept open. By rotating the handle counterclockwise the plunger moves backward and the pressure generator is filled with the test fluid. Then valve 1 is closed and valve 2 is kept open while rotating the handle clockwise and the plunger moves forward to displace the fluid into the high pressure vessel. By repeatedly doing this, the system will reach the desired pressure.

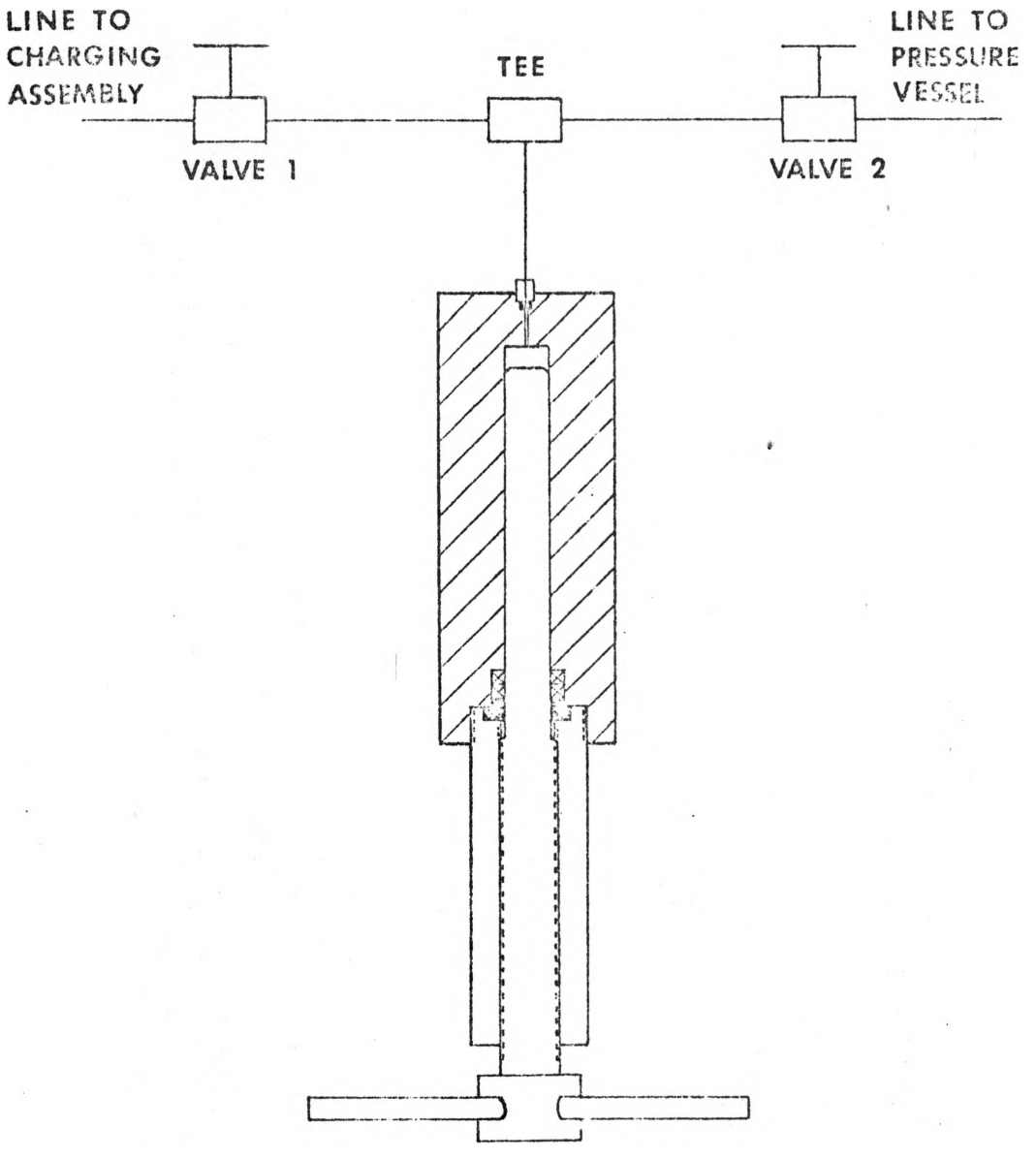

Figure 7. Pressure generator

G. Auxiliary Equipment

1. Pressure Vessel

The pressure vessel was constructed from type 316 stainless steel and rated for a maximum working pressure of 5,000 psi at 650°F. It had a 2,000 ml. capacity and served as a surge tank to smooth the pressure fluctuation in the flowing stream. It also served as a storage vessel for the high pressure fluid.

2. Valves, Tubing, and Fittings

All valves, tubing, and fittings were constructed from either type 304 or type 316 stainless steel and rated for a working pressure of 10,000 psi. Standard coned and threaded type connections were used for both 9/16" O.D. x 5/16" I.D. and 1/4" O.D. x 1/12" I.D. tubing, while taper seal connections were used for 1/4" O.D. x 1/8" I.D. tubing.

3. Vacuum System

The vacuum system consisted of a vacuum pump (Model 2AAR2, Marvac Scientific Manufacturing Company) and a mercury manometer (Model 20A10WM, Meriam Instrument Company). It had a capability of drawing to 0.1 microns and served for evacuating the closed-loop calorimeter system.

4. Charging Assembly

The charging assembly was a Pyrex glass container supported by a ring-stand. Test fluid at atmospheric pressure and room temperature was stored in the 600 ml. container. The funnel-shaped outlet of the container was connected to the low pressure side of the pressure generator. Practically no air was trapped in the charging assembly. However, a very small amount of air might dissolve in the test fluid when it was added to the container.

5. Thermocouples

A total of four bare-wire copper-constantan thermocouples were used to determine the fluid temperature in the flowmeter. Two were upstream and two downstream of the flowmeter. Since the temperature drop across the flowmeter was only about $1^{o}F$ the temperature of the fluid inside the flowmeter was taken as the arithmetic average of the temperatures measured by these thermocouples. Conax MTG-24-A4 type transducer glands were used to install these thermocouples into the flow system. The outputs of these thermocouples were also mesaured with the Leeds and Northrup differential potentiometer.

CHAPTER IV

EXPERIMENTAL PROCEDURE

A. Calibration of Thermocouples

Two thermopiles, one at the inlet and the other at the outlet of the calorimeter test section, were used to measure the temperatures of the test fluid. Each thermopile consisted of two copper-constantan thermocouples. These thermocouples were calibrated before being installed in the thermocouple fittings. A precision thermometer having resolution of $0.1^{o}C$ and the four thermocouples were immersed in the constant temperature bath using distilled water as bath fluid. The outputs of all the thermocouples agreed with each other within 0.5 microvolts at the same temperature and agreed to the International Practical Temperature Scale of 1968 (IPTS) within 2 microvolts throughout the calibration temperature range of 50^{o} to $90^{o}C$.

Due to the difficulty of selecting a suitable bath fluid which must contact the bare-wire thermocouples no calibration was made at higher temperatures. It was assumed that the thermocouples would retain the 0.5 microvolts maximum difference at higher temperatures. The calibration data for these thermocouples are shown in Table A-1 in the Appendix. The thermopile located at the inlet of the calorimeter testsection was composed of thermocouples No.1 and No.2, while that at the

outlet of the test section was composed of thermocouples No.3 and No.4. Because of this combinations minimum differences between the outputs of the thermopiles would be obtained when they were at the same temperature, thus reduced the magnitude of the probable errors in temperature difference calculations. Since the maximum discrepancy of two microvolts between the outputs of the thermocouples and the values in the IPTS tables corresponds to only 0.04°C which is less than the resolution of the thermometer, the IPTS tables are used directly to interpret the outputs of these copper-constantan thermopiles.

The chromel-alumel thermocouples used for the guard heaters were not calibrated. However, it has been observed that for each pair of these differential thermocouples at the same temperature one thermocouple always gives higher output than the other, and the differences are less than two microvolts.

The copper-constantan thermopiles located at the upstream and the downstream of the turbine flowmeter to determine the fluid temperature in the flowmeter were also calibrated against the precision thermometer over the temperature range of 50° to 90°C. The calibration data are presented in Table A-2. Deviations of the outputs of the thermocouples from the International Practical Temperature Scale of 1968 were less than 2 microvolts which corresponds to an uncertainty of only 0.04°C. Therefore the IPTS values were used to calculate the

temperature of the fluid in the flowmeter.

B. Calibration of Flowmeter

The turbine flowmeter was calibrated at the factory. The calibrating fluid (MIL-C-7024B) has a density of 0.766 grams per cubic centimeter and a viscosity of 1.446 centipoises at 80°F, the calibration temperature. The calibration data are presented in Table A-3. Calibration flow rates ranged from 0.19 to 2.10 gallons per minute. The frequencies of the corresponding sinusoidal pulses generated by the flowmeter ranged from 164 to 1811 cycles per second. Using the supplied calibration data a plot of frequencies against flow rates was drawn. The linear equation

$$V = -0.000335678 + 0.001160316\ f \qquad (11)$$

where V is the volumetric flow rate in gallons per minute and f the frequency in cycles per second, obtained through least squares method fitted all data points within $\pm 0.5\%$. Further scrutiny showed that for the range of flow rates of interest in this study, approximately 0.5 to 1.6 gallons per minute, the equation

$$V = 0.001160316\ f \qquad (12)$$

obtained by omitting the constant term from Equation 11 would fit the data within $\pm 0.2\%$.

Calibration with water was also performed for the flow-

meter. The resulting data showed that Equation 12 would give flow rates approximately 2% too low. However, it is believed that this discrepancy is caused by errors in timing and weighing and the pressure fluctuation in the pipe line. Therefore Equation 12 has been used throughout this study to calculate the volumetric flow rate.

C. Calibration of Pressure Transducers

The pressure transducers used for measuring the pressures at the inlet and the outlet of the calorimeter were calibrated by the manufacturer and were shown to have accuracies of better than 2.5 psi over the pressure range of 0 to 5,000 psi. After the pressure transducers were mounted in the system it was found that tightening of the transducers in the fittings had caused zero point shifts and therefore re-calibration became necessary.

Re-calibration was performed against a calibrated 0 - 3,000 psig Heise gauge having accuracy of 0.1% of full scale reading and resolution of 2 psi. The calibration data are presented in Table A-4. Two linear equations were obtained from the calibration data by the least squares method to show the relationships between the outputs of the transducers and the applied pressures. The pressures calculated from the equations deviate from the calibration data by no more than 2.5 psi as shown in Table A-4. Therefore these equations

have been used to calculate the actual pressures in the experimental system throughout this study.

D. Preparation of n-Pentane

The n-pentane used in this study was supplied by Phillips Petroleum Company. It was of pure grade with maximum one mole per cent impurities which consisted primarily of isopentane and cyclopentane. No attempt has been made to further purify this fluid as the effect of these impurities on the heat capacity measurements is negligible as compared with other sources of error.

The n-pentane was stored in the metal drum in which it was shipped until used to fill the charging system. The very small amount of air which might be dissolved in the n-pentane is believed to have negligible effect, if any, on the experimental results.

E. Preparation of Experimental System

Preparation of the experimental system involve the following operations:

1. Cleaning

All equipment parts which must contact the test fluid were throughly cleaned before being assembled together to form the closed-loop system. The Pyrex glass container of the

charging assembly, tubing, valves, fittings, and the high pressure vessel were cleaned using standard solution (35 ml. of saturated potassium dichromate solution mixed with 1,000 ml. of sulfuric acid) and rinsed with distilled water to remove all dirt and grease. The calorimeter proper was cleaned by passing detergent solution through it and rinsed with distilled water. The pressure generator and the high pressure turbine pump were disassembled into parts and cleaned using acetone and n-pentane. The intensifying cylinder of the high pressure pump was cleaned and filled with n-pentane.

2. Evacuation

The vacuum pump was started to remove the air trapped in the closed system after all equipment parts had been put together. Although the vacuum pump is capable of achieving an ultimate absolute pressure of 0.0001 mm Hg as specified by the manufacturer, the system pressure could only reach 20 mm Hg because of the diffusion of n-pentane from the intensifying cylinder to the inside of the pump through the stuffing box.

3. Pressure Test

After the system was first assembled it was filled with n-pentane and pressurized to 3,000 psig at room temperature. The system pressure dropped about 15 psi after twelve hours. This leakage, believed to be through the stuffing box of the

turbine pump, was considered negligible. After several runs leakage was found in the calorimeter and this was eradicated before any further experiment was conducted.

F. Operating Procedure

The actual experiment began when the system was filled with n-pentane and the constant temperature bath was heated to a temperature a few degrees Fahrenheit lower than the desired average temperature of the calorimeter. The high pressure turbine pump was then started to circulate the test fluid at constant flow rate while at the same time the D.C. power supply was turned on to apply electrical energy to the main heater of the calorimeter. All five autotransformers were also turned on and regulated manually to apply appropriate amount of electrical energy to the guard heaters. The temperature gradients across the insulations between the main heater and the outer tube, as well as those along the axial direction at the ends of the calorimeter, were reduced to a very small amount. The temperature gradient was considered to be small enough when the output of the corresponding differential thermocouple was less than one microvolt. In terms of temperature difference, this is equivalent to approximately $0.025^{\circ}C$. During these operations the pressure generator was also manipulated in order to reach the desired system pressure.

The system was considered to have reached a steady state when the outputs of the main thermopiles and the pressure transducers remained constant for at least five minute. Outputs of the differential thermocouples were checked during the five minutes interval to make sure all of them were within the one microvolt tolerance. Since the heat losses were reduced to a minimum amount by the use of the guard heaters, the electrical power applied to the main heater was considered entirely to provide the heating of the test fluid. No corrections for the heat losses were needed.

The frequency of the pulses generated by the flowmeter was displayed by the frequency counter. Constant flow rate in the system was assured by the virtually constant frequency shown. The voltage across and the current through the main heater, the temperatures of the fluid at the inlet and outlet of the calorimeter test section, and the temperatures of the fluid entering and leaving the flowmeter were measured at this time using the differential potentiometer.

Then the thermo-regulator of the constant temperature bath was set at a higher temperature. The system pressure was kept constant by releasing the fluid through the pressure generator as the system temperature was increasing. The output of the pressure transducer located at the upstream side of the calorimeter was measured from time to time to ensure that the pressure at that point was always the same throughout the

isobaric run. The measurement procedures were repeated when the system reached the new steady state. After enough data had been obtained for one pressure level, the system pressure was changed and experiment was conducted at the new pressure level in a similar manner.

It was necessary to replace the "O" ring in the stuffing box of the high pressure pump after, and sometimes during, each isobaric run as the wear and tear of the "O" ring caused leakage through the stuffing box. The system was cooled down to room temperature and the pressure was released before taking the pump apart to do the replacement work. It was also necessary to change the bath fluid from distilled water to silicone oil or from silicone oil to distilled water from time to time depending on whichever was suitable for the temperature region of interest.

G. Calculation of Heat Capacity Values

The heat capacity values of n-pentane were calculated from the measured quantities by using the equation

$$C_p = 366.727 \times \frac{E \cdot I \cdot v}{f(t_2 - t_1)} - \frac{P_2 - P_1}{t_2 - t_1} \left(\frac{\partial H}{\partial P}\right)_{t_2} \qquad (13)$$

where E = voltage across the main heater, volts

I = current through the main heater, amperes

v = specific volume of n-pentane at flowmeter temperature, ft^3/lb

f = frequency of the flowmeter output signal, Hz

t = temperature of n-pentane, ^{o}F

P = pressure of n-pentane, psia

$\frac{\partial H}{\partial P}$ = enthalpy-pressure coefficient, Btu/lb psi

C_p= heat capacity of n-pentane at the average temperature of t_1 and t_2 and the pressure P_1, Btu/lb ^{o}F

Subscripts 1 and 2 refer to, respectively, the inlet and outlet of the calorimeter proper. The constant is a conversion factor.

E and I were obtained directly from the potentiometer readings. The temperatures t_1 and t_2 were obtained by converting the outputs of the thermopiles into temperatures using International Practical Temperature Scale of 1968. The specific volumes as well as the enthalpy-pressure coefficients were obtained by interpolation of the data presented by Sage and Lacey(61). Since the enthalpy-pressure coefficients were very small in the region of this study, a 10% error in $\frac{P_1-P_2}{t_2-t_1}$ value would contribute an error of only 0.025% of the heat capacity value. Therefore the values of $\frac{P_1-P_2}{t_2-t_1}$ have been taken as 0.5 psi/^{o}F which is very close to the actual values throughout the calculation.

The derivation of Equation 13 as well as a sample calculation using this equation is presented in Appendix B.

CHAPTER V

EXPERIMENTAL RESULTS AND TREATMENT OF DATA

In order to check the reliability of the calorimeter system, the isobaric heat capacity of water was initially determined. The calorimeter was connected to the water main. Water at room temperature flowed through the calorimeter and the flowmeter, then discharged to the atmosphere. The pressure in the calorimeter was not more than a few pounds per square inch higher than atmospheric pressure as indicated by a mercury manometer. The experimental data are included in Table I. The results obtained agree with the literature data for saturated water (46) at the experimental temperature within 1%. Since the flowmeter uses carbon steel bearing, no attempts were made to test the calorimeter using water at high temperature and/or high pressure as the bearing would probably be damaged at these conditions. However, it is believed that the calorimeter system has generated reliable data and with some revisions it will be suitable for the measurement of heat capacities of fluid at more severe conditions.

Experimental data have been obtained for the isobaric heat capacity of n-pentane in the dense liquid region. A total of 20 runs were made over the temperature range of 130° to 300°F, at approximately 15°F to 20°F intervals, for pressures of 400, 500, 800, 1,000, 1,500, 2,000, and 3,000 psia. A total of 95

data points have been obtained. In Table II the experimental results are presented in raw data form.

In order to present heat capacity values for n-pentane at various temperatures and pressures for the entire region of this study, interpolation methods were applied. The values of $C_p - C_p^o$, where C_p is the experimental heat capacity and C_p^o the ideal gas heat capacity of n-pentane at the corresponding temperature for C_p, were obtained and and equations having the form

$$(C_p - C_p^o)_{calc} = \alpha (T_R - \gamma)^2 + \beta \qquad (14)$$

were used to fit these values. The coefficients α, β, and γ are functions of pressure and were obtained by the least squares method by the use of computer. The functional form of α, β, and γ are presented in Table III.

Comparisons of the experimental heat capacity values with the smoothed values calculated by using Equation 14 are included in Table II. For the entire set of data, an average percentage difference of 0.29% and a standard error of estimate of 0.0025 Btu/lb ^oF were obtained. These results indicate that the error in the smoothed heat capacity values are within the experimental error and that Equation 14 can be used to calculate the heat capacity of n-pentane at pressures and temperatures within the region of this study.

Table IV shows heat capacity values for n-pentane cal-

culated using Equation 14 at 10°F intervals from 140°F to 300°F for ten pressures between 400 and 3,000 psia. Curves showing the smoothed heat capacity values as functions of temperature are presented in Figures 8 through 14 for the seven experimental pressures.

TABLE I

Experimental Heat Capacity Data for Water

W Btu/sec	t_1 °F	t_2 °F	m lb/sec	t_{ave} °F	C_p Btu/lb°F
0.5653	69.05	74.17	0.1103	71.61	0.9996
0.5648	68.86	73.97	0.1103	71.42	1.0027

Calorimeter inlet pressure ≈ 5 psig

C_p are calculated through Equation 13 neglecting the pressure correction term

Literature value: C_p = 0.9992 Btu/lb°F at 72°F. (Ref. 46)

TABLE II

Experimental Results for n-Pentane

P_1 psia	W Btu/sec	m lb/sec	t_1 °F	t_2 °F	Correction Btu/lb°F	t_{ave} °F	C_p Btu/lb°F	$C_{p_{calc}}$ Btu/lb°F	%Diff.
400	0.5569	0.0800	128.63	140.26	0.0010	134.44	0.5989	0.6005	0.28
400	0.5567	0.0798	145.74	157.29	0.0009	151.51	0.6048	0.6062	0.24
400	0.5552	0.0789	169.89	181.16	0.0007	175.52	0.6254	0.6174	-1.28
400	0.5542	0.0778	182.34	193.72	0.0006	188.03	0.6263	0.6246	-0.27
400	0.5540	0.0772	193.38	204.71	0.0005	199.05	0.6342	0.6318	-0.37
400	0.5550	0.0768	212.17	223.39	0.0003	217.78	0.6445	0.6458	0.19
400	0.5559	0.0787	212.62	223.51	0.0003	218.06	0.6490	0.6460	-0.47
400	0.5537	0.0760	213.04	224.33	0.0003	218.68	0.6457	0.6465	0.12
400	0.5545	0.0754	226.97	238.18	0.0001	232.58	0.6559	0.6584	0.37
400	0.5533	0.0744	230.17	241.43	0.0001	235.80	0.6608	0.6613	0.08
400	0.5540	0.0738	244.11	255.30	-0.0003	249.70	0.6705	0.6746	0.62
400	0.5531	0.0716	255.62	266.87	-0.0005	261.24	0.6863	0.6866	0.04
400	0.5536	0.0725	260.86	272.00	-0.0007	266.43	0.6848	0.6923	1.10
400	0.5519	0.0698	270.67	281.93	-0.0009	276.30	0.7017	0.7035	0.27
400	0.5516	0.0685	280.48	291.71	-0.0014	286.09	0.7156	0.7153	-0.03
400	0.5525	0.0682	282.41	293.66	-0.0015	288.03	0.7185	0.7177	-0.11
400	0.5513	0.0665	295.05	306.27	-0.0025	300.66	0.7367	0.7339	-0.38

TABLE II (Continued)

P_1 psia	W Btu/sec	m lb/sec	t_1 °F	t_2 °F	Correction Btu/lb°F	t_{ave} °F	C_p Btu/lb°F	$C_{p_{calc}}$ Btu/lb°F	%Diff.
500	0.5571	0.0820	133.41	144.76	0.0010	139.08	0.5993	0.6010	0.28
500	0.5564	0.0804	151.36	162.76	0.0009	157.06	0.6083	0.6075	-0.14
500	0.5554	0.0806	169.91	181.06	0.0008	175.48	0.6192	0.6160	-0.51
500	0.5548	0.0793	188.29	199.44	0.0006	193.86	0.6281	0.6265	-0.25
500	0.5543	0.0779	206.69	217.80	0.0004	212.24	0.6411	0.6389	-0.34
500	0.5528	0.0772	211.10	222.20	0.0004	216.65	0.6447	0.6422	-0.39
500	0.5544	0.0772	211.95	223.13	0.0004	217.54	0.6427	0.6429	0.03
500	0.5560	0.0789	212.83	223.75	0.0004	218.29	0.6457	0.6435	-0.34
500	0.5515	0.0760	225.56	236.64	0.0002	231.10	0.6555	0.6538	-0.26
500	0.5544	0.0758	226.89	238.11	0.0002	232.50	0.6517	0.6550	0.49
500	0.5507	0.0748	241.86	252.93	0.0001	247.39	0.6655	0.6683	0.42
500	0.5539	0.0744	243.91	255.04	-0.0001	249.47	0.6688	0.6702	0.21
500	0.5504	0.0732	260.28	271.30	-0.0005	265.79	0.6822	0.6865	0.63
500	0.5534	0.0727	260.80	271.98	-0.0005	266.39	0.6799	0.6871	1.06
500	0.5514	0.0718	275.20	286.20	-0.0010	280.70	0.6970	0.7027	0.83
500	0.5527	0.0684	284.11	295.38	-0.0013	289.74	0.7152	0.7132	-0.28
500	0.5528	0.0698	290.50	301.35	-0.0017	295.93	0.7276	0.7207	-0.96
800	0.5568	0.0807	128.70	140.32	0.0011	134.51	0.5945	0.5972	0.44
800	0.5566	0.0806	145.77	157.30	0.0010	151.54	0.6000	0.6025	0.42

TABLE II (Continued)

P_1 psia	W Btu/sec	m lb/sec	t_1 °F	t_2 °F	Correction Btu/lb°F	t_{ave} °F	C_p Btu/lb°F	$C_{p_{calc}}$ Btu/lb°F	%Diff.
800	0.5548	0.0801	162.50	173.90	0.0009	168.20	0.6079	0.6091	0.20
800	0.5542	0.0797	181.26	192.52	0.0008	186.89	0.6186	0.6181	-0.08
800	0.5539	0.0788	197.83	209.06	0.0007	203.45	0.6268	0.6274	0.10
800	0.5547	0.0779	211.96	223.12	0.0005	217.54	0.6388	0.6363	-0.39
800	0.5547	0.0761	226.43	237.69	0.0004	232.06	0.6475	0.6465	-0.16
800	0.5542	0.0752	243.53	254.72	0.0001	249.14	0.6581	0.6598	0.26
800	0.5531	0.0739	260.59	271.76	-0.0002	266.18	0.6703	0.6744	0.60
800	0.5527	0.0711	278.66	289.91	-0.0006	284.28	0.6904	0.6914	0.15
800	0.5522	0.0694	294.13	305.32	-0.0011	299.72	0.7096	0.7072	-0.35
1000	0.5573	0.0825	133.35	144.73	0.0011	139.04	0.5949	0.5967	0.30
1000	0.5564	0.0814	151.29	162.68	0.0010	156.99	0.6015	0.6028	0.21
1000	0.5556	0.0805	169.96	181.33	0.0009	175.64	0.6080	0.6105	0.41
1000	0.5548	0.0806	188.33	199.48	0.0008	193.90	0.6178	0.6194	0.26
1000	0.5543	0.0793	206.71	217.83	0.0007	212.27	0.6291	0.6297	0.10
1000	0.5533	0.0784	211.33	222.48	0.0006	216.90	0.6338	0.6325	-0.19
1000	0.5561	0.0801	212.87	223.83	0.0006	218.35	0.6342	0.6334	-0.11
1000	0.5517	0.0772	225.49	236.60	0.0005	231.05	0.6435	0.6417	-0.28
1000	0.5554	0.0786	233.22	244.24	0.0004	238.73	0.6420	0.6470	0.78
1000	0.5504	0.0763	241.50	252.55	0.0003	247.02	0.6530	0.6530	-0.00

TABLE II (Continued)

P_1 psia	W Btu/sec	m lb/sec	t_1 °F	t_2 °F	Correction Btu/lb°F	t_{ave} °F	C_p Btu/lb°F	$C_{p_{calc}}$ Btu/lb°F	%Diff.
1000	0.5507	0.0750	260.25	271.24	0.0000	265.74	0.6681	0.6676	-0.08
1000	0.5516	0.0736	275.53	286.47	-0.0003	281.00	0.6851	0.6806	-0.66
1000	0.5529	0.0722	290.57	301.53	-0.0006	296.05	0.6984	0.6943	-0.60
1500	0.5577	0.0822	133.44	144.94	0.0011	139.19	0.5914	0.5922	0.13
1500	0.5563	0.0821	151.40	162.65	0.0011	157.02	0.6035	0.5986	-0.81
1500	0.5556	0.0813	170.07	181.39	0.0010	175.73	0.6050	0.6062	0.21
1500	0.5548	0.0818	188.28	199.37	0.0009	193.82	0.6126	0.6145	0.31
1500	0.5543	0.0811	206.85	217.81	0.0008	212.33	0.6241	0.6240	-0.02
1500	0.5542	0.0785	209.75	221.04	0.0008	215.39	0.6262	0.6256	-0.09
1500	0.5537	0.0791	211.27	222.37	0.0008	216.82	0.6311	0.6264	-0.75
1500	0.5561	0.0806	212.91	223.96	0.0008	218.44	0.6256	0.6273	0.27
1500	0.5517	0.0783	225.45	236.51	0.0007	230.98	0.6377	0.6344	-0.51
1500	0.5535	0.0775	225.58	236.82	0.0007	231.20	0.6358	0.6345	-0.20
1500	0.5507	0.0774	241.02	252.13	0.0005	246.57	0.6407	0.6439	0.50
1500	0.5524	0.0765	241.22	252.43	0.0005	246.82	0.6447	0.6440	-0.11
1500	0.5509	0.0763	259.53	270.55	0.0003	265.04	0.6549	0.6560	0.16
1500	0.5534	0.0748	277.33	288.41	0.0001	282.87	0.6678	0.6685	0.11
1500	0.5528	0.0738	290.66	301.70	-0.0001	296.18	0.6778	0.6785	0.10
2000	0.5575	0.0826	133.44	144.92	0.0012	139.18	0.5894	0.5882	-0.20

TABLE II (Continued)

P_1 psia	W Btu/sec	m lb/sec	t_1 ^oF	t_2 ^oF	Correction Btu/lb^oF	t_{ave} ^oF	C_p Btu/lb^oF	$C_{p_{calc}}$ Btu/lb^oF	%Diff.
2000	0.5564	0.0823	151.31	162.67	0.0012	156.99	0.5965	0.5950	-0.25
2000	0.5558	0.0814	170.08	181.38	0.0011	175.73	0.6051	0.6028	-0.37
2000	0.5549	0.0808	188.24	199.46	0.0010	193.85	0.6128	0.6110	-0.29
2000	0.5533	0.0799	205.32	216.52	0.0010	210.92	0.6190	0.6194	0.05
2000	0.5544	0.0801	206.77	217.94	0.0010	212.36	0.6201	0.6201	0.00
2000	0.5531	0.0788	223.13	234.32	0.0008	228.72	0.6284	0.6286	0.03
2000	0.5525	0.0777	242.12	253.24	0.0007	247.68	0.6398	0.6391	-0.10
2000	0.5522	0.0768	256.21	267.32	0.0006	261.77	0.6477	0.6474	-0.05
2000	0.5517	0.0766	272.05	283.02	0.0004	277.54	0.6575	0.6571	-0.06
2000	0.5515	0.0753	289.61	300.55	0.0003	295.08	0.6696	0.6684	-0.17
3000	0.5570	0.0847	129.09	140.32	0.0013	134.71	0.5874	0.5874	0.00
3000	0.5558	0.0837	148.26	159.48	0.0013	153.87	0.5933	0.5939	0.11
3000	0.5548	0.0827	168.19	179.40	0.0012	173.80	0.5993	0.6013	0.33
3000	0.5543	0.0817	185.86	197.04	0.0012	191.45	0.6084	0.6084	0.00
3000	0.5535	0.0806	205.48	216.64	0.0011	211.06	0.6167	0.6169	0.03
3000	0.5545	0.0797	209.35	220.63	0.0011	214.99	0.6176	0.6187	0.17
3000	0.5541	0.0789	225.42	236.67	0.0011	231.04	0.6260	0.6262	0.03

TABLE II (Contiuned)

P_1 psia	W Btu/sec	m lb/sec	t_1 ^oF	t_2 ^oF	Correction Btu/lb^oF	t_{ave} ^oF	C_p Btu/lb^oF	$C_{p_{calc}}$ Btu/lb^oF	%Diff.
3000	0.5540	0.0778	241.11	252.34	0.0010	246.73	0.6349	0.6339	-0.15
3000	0.5536	0.0770	257.10	268.31	0.0009	262.71	0.6424	0.6422	-0.03
3000	0.5531	0.0762	273.33	284.50	0.0008	278.92	0.6507	0.6511	0.05
3000	0.5525	0.0754	289.48	300.61	0.0007	295.04	0.6595	0.6603	0.12

C_p are calculated using Equation 13 while $C_{p_{calc}}$ are calculated through Equation 14.

$$\%\text{Diff.} = \frac{C_{p_{calc}} - C_p}{C_p} \times 100$$

TABLE III

Coefficients of Equation 14

	i = 1	i = 2	i = 3
a_i	3.03332	-0.17768×10^{-2}	0.335543×10^{-6}
b_i	0.16399	-0.18618×10^{-4}	0.264286×10^{-8}
c_i	0.74125	0.50351×10^{-4}	-0.262730×10^{-8}

Equation 14:

$$(C_p - C_p^o)_{calc} = \alpha (T_R - \gamma)^2 + \beta$$

where $\alpha = \alpha(P) = a_1 + a_2 P + a_3 P^2$

$\beta = \beta(P) = b_1 + b_2 P + b_3 P^2$

$\gamma = \gamma(P) = c_1 + c_2 P + c_3 P^2$

P are pressures in psia and C_p^o, the ideal gas heat capacity values, are obtained from API Technical Data Book(2).

TABLE IV

Smoothed Values of Isobaric Heat Capacity of n-Pentane, Btu/lb°F

Temp., °F	Pressure, psia									
	400	500	600	800	1000	1250	1500	2000	2500	3000
140	0.602	0.601	0.600	0.599	0.597	0.595	0.592	0.588	0.588	0.588
150	0.606	0.605	0.604	0.602	0.600	0.598	0.596	0.592	0.592	0.592
160	0.610	0.609	0.608	0.606	0.604	0.602	0.600	0.596	0.595	0.595
170	0.615	0.613	0.612	0.610	0.608	0.606	0.604	0.600	0.599	0.599
180	0.620	0.618	0.617	0.615	0.612	0.610	0.608	0.605	0.604	0.604
190	0.626	0.624	0.623	0.620	0.617	0.615	0.613	0.609	0.608	0.608
200	0.632	0.630	0.629	0.625	0.623	0.620	0.618	0.614	0.612	0.612
210	0.640	0.637	0.635	0.631	0.628	0.625	0.623	0.619	0.617	0.616
220	0.648	0.645	0.642	0.638	0.634	0.631	0.628	0.624	0.622	0.621
230	0.656	0.653	0.650	0.645	0.641	0.637	0.634	0.629	0.627	0.626
240	0.665	0.662	0.658	0.653	0.648	0.643	0.640	0.635	0.632	0.631
250	0.675	0.671	0.667	0.660	0.655	0.650	0.646	0.640	0.637	0.636
260	0.685	0.681	0.676	0.669	0.663	0.657	0.653	0.646	0.643	0.641
270	0.696	0.691	0.686	0.678	0.671	0.664	0.659	0.652	0.648	0.646
280	0.708	0.702	0.697	0.687	0.680	0.672	0.666	0.659	0.654	0.652
290	0.720	0.714	0.708	0.697	0.689	0.680	0.674	0.665	0.660	0.657
300	0.733	0.726	0.719	0.707	0.698	0.689	0.681	0.672	0.666	0.663

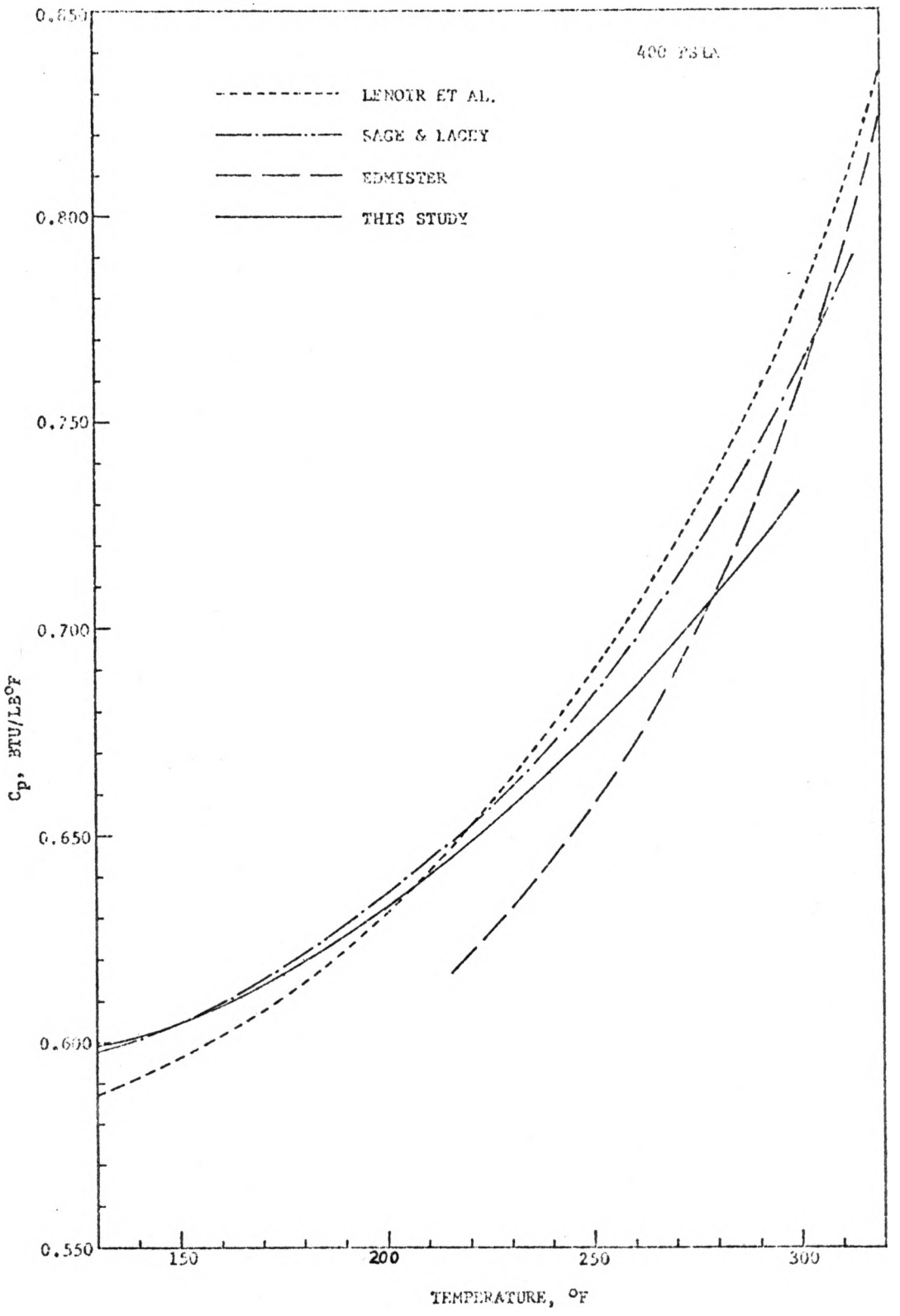

Figure 8. Comparison of experimental results for n-pentane with calculated values

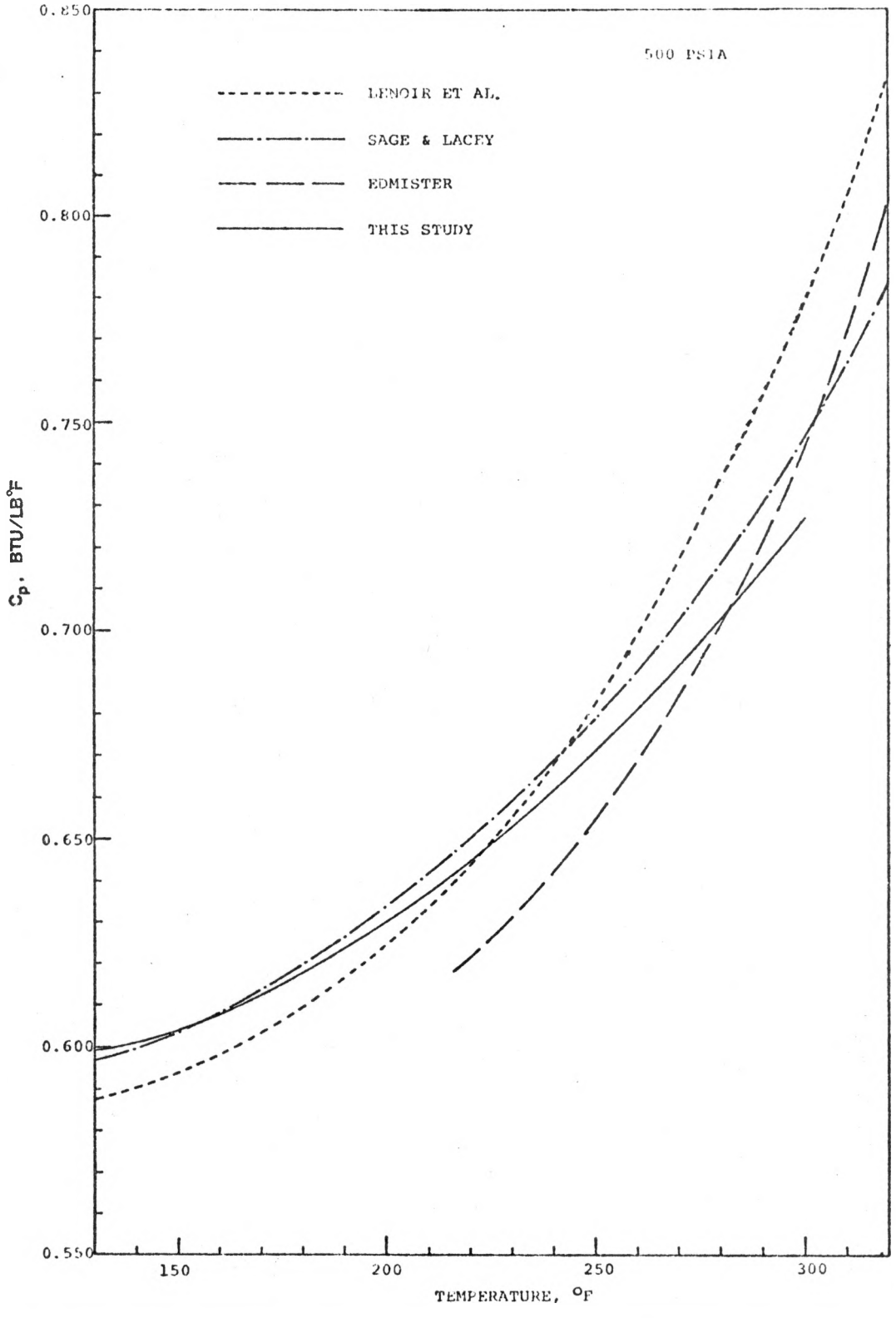

Figure 9. Comparison of experimental results for n-pentane with calculated values

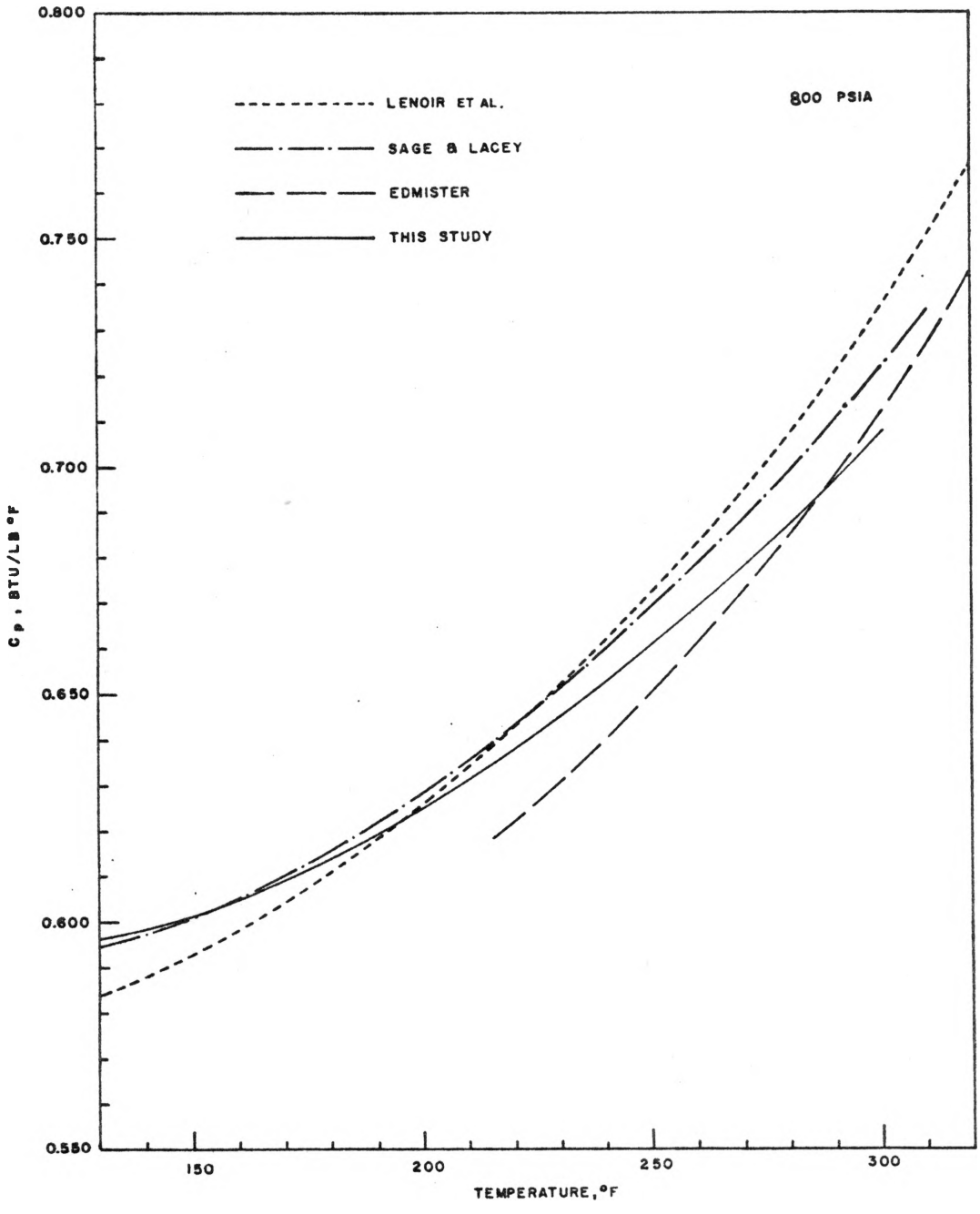

Figure 10. Comparison of experimental results for n-pentane with calculated values

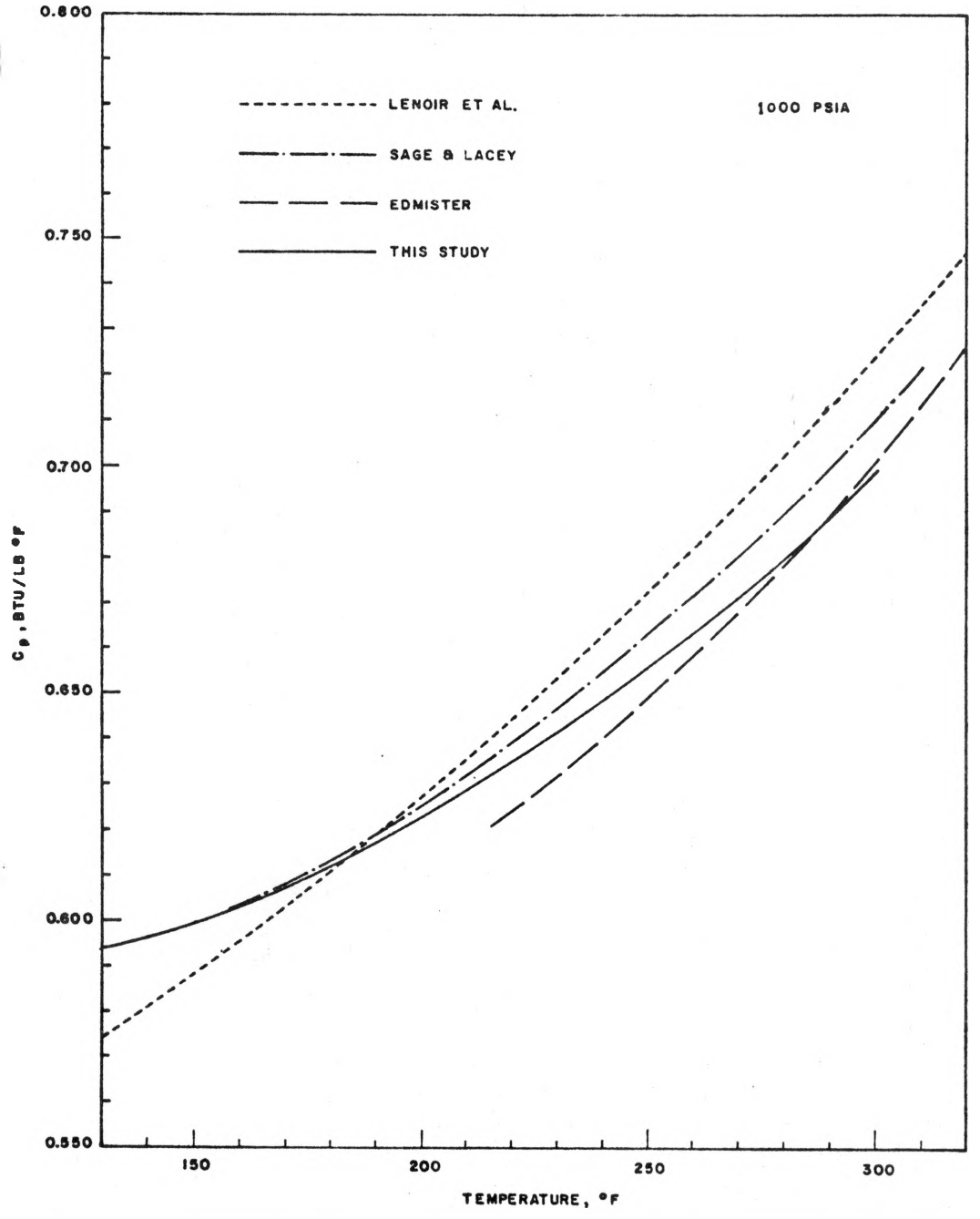

Figure 11. Comparison of experimental results for n-pentane with calculated values

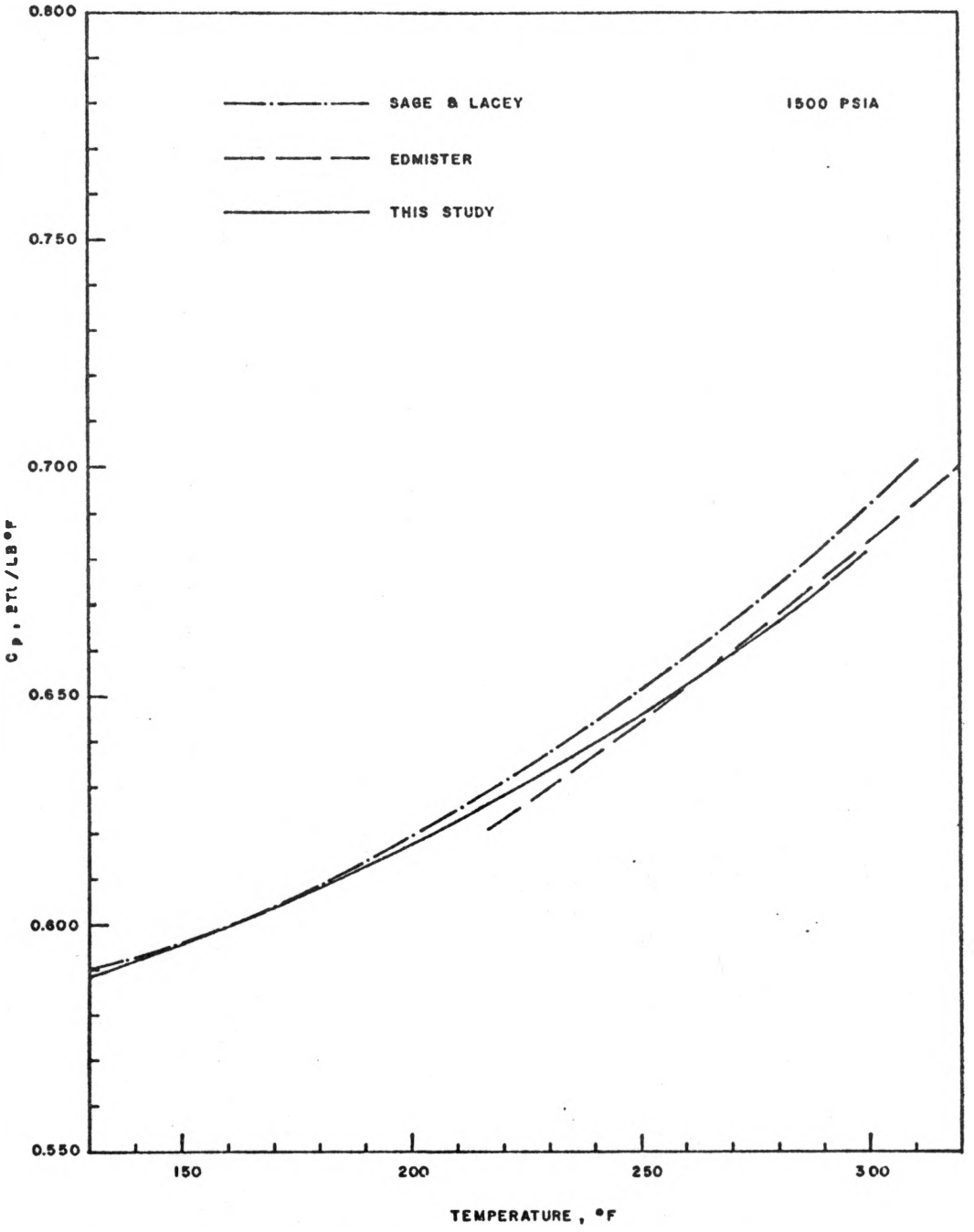

Figure 12. Comparison of experimental results for n-pentane with calculated values

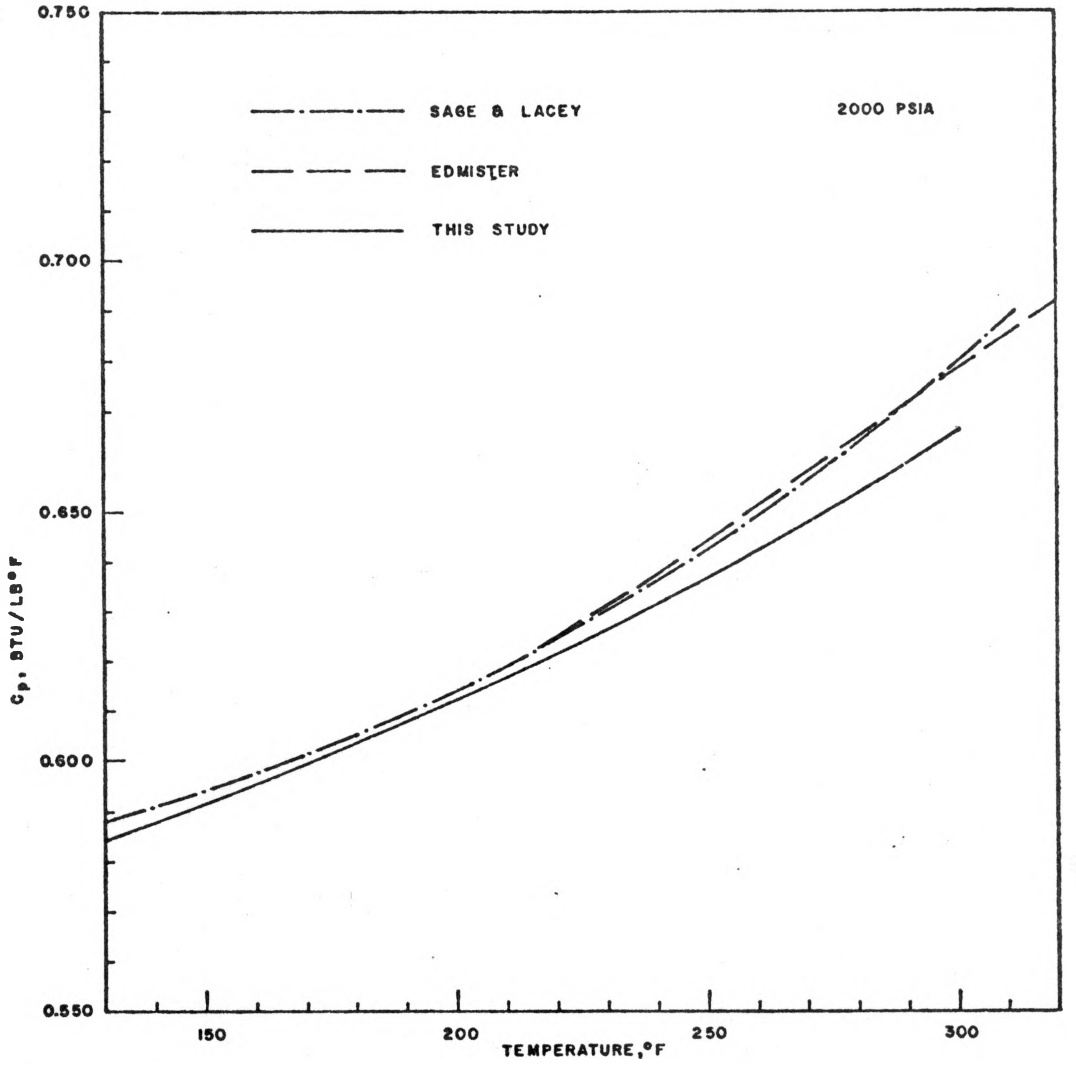

Figure 13. Comparison of experimental results for n-pentane with calculated values

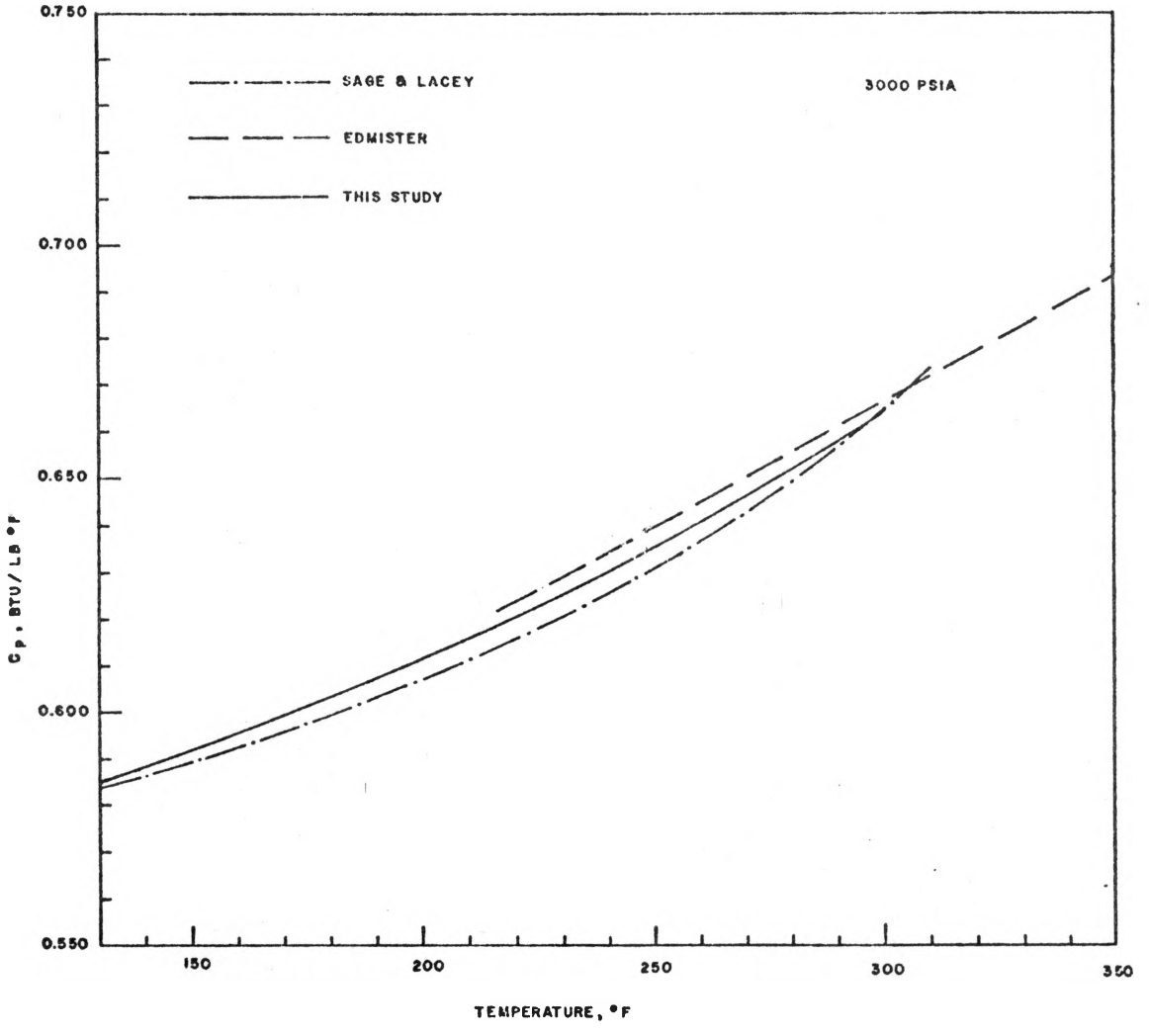

Figure 14. Comparison of experimental results for n-pentane with calculated values

CHAPTER VI

ERROR ANALYSIS

The experimental errors in the measured isobaric heat capacities of n-pentane are estimated as follows:

The isobaric heat capacity, C_p, is calculated using the equation (see Appendix B)

$$C_p = \frac{W}{\dot{m}\,\Delta t} - \frac{\Delta P}{\Delta t}\left(\frac{\partial H}{\partial P}\right)_{t_2} \tag{15}$$

where W is the electric power input, $\dot{m}$ the mass flow rate, Δt the temperature rise of the fluid in the calorimeter, ΔP the pressure drop of the fluid through the calorimeter, and $\left(\frac{\partial H}{\partial P}\right)_{t_2}$ the enthalpy-pressure coefficient of the fluid at the system pressure and the temperature t_2. It has been shown that the second term is very small compared with the first term hence the error in the second term will not be discussed.

The total differential of C_p can be written as

$$dC_p = \left(\frac{\partial C_p}{\partial W}\right)dW + \left(\frac{\partial C_p}{\partial \dot{m}}\right)d\dot{m} + \left(\frac{\partial C_p}{\partial \Delta t}\right)d\Delta t \tag{16}$$

This equation can be reduced to

$$\frac{dC_p}{C_p} = \frac{dW}{W} - \frac{d\dot{m}}{\dot{m}} - \frac{d\Delta t}{\Delta t} \tag{17}$$

The maximum error estimated for C_p will be the sum of the uncertainty in the measurements of the power input, the mass flow rate, and the temperature rise. Since the power input is the product of the voltage applied to the main heater and

the current through it, the uncertainty of the power input is the sum of the uncertainty in the measurements of the voltage, E, and the current, I. The uncertainty in the measurements of volumetric flow rate and the probable error of n-pentane density data, ρ, taken from the work of Sage and Lacey (61), constitute the uncertainty of the mass flow rate.

Rewrite Equation 17 in the form

$$\frac{dC_p}{C_p} = \left(\frac{dE}{E} + \frac{dI}{I}\right) - \left(\frac{dV}{V} + \frac{d\rho}{\rho}\right) - \frac{d\Delta t}{\Delta t} \qquad (18)$$

The maximum possible uncertainty in the isobaric heat capacity is therefore

$$\frac{dC_p}{C_p} = \left|\frac{dE}{E}\right| + \left|\frac{dI}{I}\right| + \left|\frac{dV}{V}\right| + \left|\frac{d\rho}{\rho}\right| + \left|\frac{d\Delta t}{\Delta t}\right| \qquad (19)$$

The voltage drop across the calorimeter main heater was measured with the differential potentiometer. Referring to Figure 4, there were no errors to be considered for the leads. The error in the voltage measurement is therefore the summation of the error in the potentiometer reading at the voltage range and the stability of the D.C. voltage applied by the power supply:

$$\frac{dE}{E} = 0.008\% + 0.05\% = 0.058\%$$

Similarly, the error in the current measurement is the summation of the accuracy of the current shunt box and the accuracy of the potentiometer reading:

$$\frac{dI}{I} = 0.02\% + 0.0016\% = 0.0216\%$$

The equation used for calculating the volumetric flow rate from the frequency of the output signal of the flowmeter has an accuracy of 0.2% in the flow rate range of this study. The frequency counter has an accuracy of ± 1 count, which is equal to 0.11% at the frequency range of this study. The error in flow rate measurement is consequently

$$\frac{dV}{V} = 0.2\% + 0.11\% = 0.31\%$$

The error in the density value is due to interpolation of the density data of Sage and Lacey (61), and the error in the original density data. Sage and Lacey (61) claimed that their data have accuracy of better than 0.25% except in the neighborhood of the critical region where larger error may exist. It is believed that the interpolation of the data of Sage and Lacey (61) would produce errors no larger than 0.05% for the region of this study. The uncertainty of the density values is

$$\frac{d\rho}{\rho} = 0.25\% + 0.05\% = 0.30\%$$

The non-ideality of the thermocouples resulted in an error of 0.5 microvolts between the outputs of the thermocouples. The error in the potentiometer readings was 0.5 microvolts. The maximum probable error in the temperature difference is the sum of these two quantities which is equivalent to $0.04^{\circ}F$. The temperature differences were approximately $11^{\circ}F$ during the experiments. Therefore the percent

error is

$$\frac{d\Delta t}{\Delta t} = \frac{0.04}{11} \times 100\% = 0.36\%$$

The maximum possible uncertainty in the isobaric heat capacity of n-pentane is calculated to be

$$\frac{dC_p}{C_p} = 0.058\% + 0.022\% + 0.31\% + 0.30\% + 0.36\%$$
$$= 1.05\%$$

Since the above figure represents the error which would exist for the worst condition, in actuality some errors may cancel out and the accuracy of the experimental results is believed to be better than 1%. The probable error in C_p, calculated as the square root of the sum of squares of the individual uncertainties discussed above, has the value of 0.56%.

It should be noted that it was very difficult to reach the steady state and to obtain a point, and that the room temperature was not controlled, consequently the precision was of the same order of magnitude as the experimental error.

CHAPTER VII

COMPARISON OF RESULTS WITH CALCULATED VALUES

There are no experimental heat capacity data for n-pentane for the region of this investigation. In order to determine the accuracy of the experimental results obtained in this study, it is necessary to compare the data with values calculated by various methods.

Theoretically, the isobaric heat capacity can be derived by simply taking the derivative of the enthalpy with respect to temperature at constant pressure or from experimental P-V-T data by using rigorous thermodynamic relationship. Since the differentiation of enthalpy with respect to temperature is a straight-forward method to obtain heat capacity values, it is of interest to compare the enthalpy values provided by different investigators. Therefore, enthalpy values of n-pentane have been calculated from the isothermal enthalpy difference values presented by Sage and Lacey (61), from the generalized equation presented by Yen and Alexander (77), and from the generalized tables prepared by Curl and Pitzer (16), and are compared with the experimental values of Lenoir, Robinson, and Hipkin (32).

A. Comparison of Enthalpy Values of n-Pentane

Sage and Lacey (61) presented the calculated isothermal

enthalpy difference values, $\Delta H(t,P)$, for n-pentane at seven temperatures between 100° and 460°F over the pressure range of 0 to 10,000 psia. The enthalpy values can be calculated using the simple equation

$$H(t,P) = H^{o}(t) - \Delta H(t,P) \tag{20}$$

where $H(t,P)$ is the enthalpy at temperature t and pressure P and $H^{o}(t)$ the corresponding ideal gas enthalpy.

The equation presented by Yen and Alexander (77) for the reduced enthalpy departure of compressed liquids in the z_c = 0.27 group (z_c= 0.269 for n-pentane) is

$$\begin{aligned}\frac{\tilde{H}^{o}-\tilde{H}}{T_c} = &-0.1368774\ (P_R-4.664)\\ &-14.56975\ (T_R-0.79749)\\ &-7.812724\ (T_R-0.79749)^2\\ &-0.1642482\ (T_R-0.79749)(P_R-4.664)\\ &+1.036851\ \ln(P_R)\\ &+4.463472\ \ln(P_R)\ \ln(T_R)\\ &+4.525831\ \ln(P_R)\left[\ln(T_R)\right]^2\\ &+10.86085\end{aligned} \tag{21}$$

where $0.01 < P_R < 30$ and $0.5 < T_R < 1.0$. The enthalpy values of n-pentane are obtained through the equation

$$H = H^{o} - \frac{T_c}{M}\left(\frac{\tilde{H}^{o}-\tilde{H}}{T_c}\right) \tag{22}$$

where T_c is the critical temperature and M the molecular weight of n-pentane.

To calculated the enthalpy values from the tables prepared by Curl and Pitzer (16) for the reduced enthalpy departure of non-polar fluids, both $(\frac{\tilde{H}^o-\tilde{H}}{RT_c})^{(o)}$ and $(\frac{\tilde{H}^o-\tilde{H}}{RT_c})^{(1)}$ are interpolated from the tables, and the reduced enthalpy departures are calculated using Equation 3. For n-pentane the acentric factor, ω, has the value of 0.252 (55). The enthalpy values of n-pentane are calculated through the equation

$$H = H^o - \frac{RT_c}{M}(\frac{\tilde{H}^o-\tilde{H}}{RT_c}) \qquad (23)$$

where R is the gas constant.

The ideal gas enthalpy values, H^o, which are required in all of the above calculations are obtained from API Technical Data Book (2). Consequently, the calculated enthalpy values have a enthalpy basis of zero for the saturated liquid at -200^oF.

The enthalpy values of n-pentane presented by Brydon, Walen, and Canjar (9) were calculated from the experimental P-V-T data of Sage and Lacey (61) for temperatures of 100^o to 212^oF and of Li and Canjar (36) for temperatures of 212^o to 347^oF. The enthalpy values have a basis of zero enthalpy for the ideal gas at 0^oR. No attempt has been made to convert the enthalpy basis to that used in the API Technical Data Book because it is felt that additional errors would be introduced. However, the enthalpy values from this reference have been smoothed and differentiated with respect to tem-

perature to obtain heat capacity values, as discussed below.

The only experimental enthalpy values for n-pentane are those presented by Lenoir, Robinson, and Hipkin (32). These investigators used a flow calorimeter to measure the enthalpy of n-pentane above a datum of liquid at 75°F and the system pressure. Through conversions of the enthalpy basis they reported the enthalpy values on a basis of zero enthalpy at -200°F and saturated liquid.

Since the differences between the calculated enthalpy values and the experimental data reported by Lenoir et al. (32) are not large enough to allow comparisons by plotting, the enthalpy values are presented in tabular form as shown in Table V. It can be seen that generally the values are in good agreement except for temperatures near the critical point where larger differences are observed. It should be noted that although the differences between the enthalpy values obtained through various methods are small, significant deviations should be expected for the heat capacity values which are the slopes of the enthalpy-temperature curves at constant pressure.

B. Comparison of Heat Capacity Values of n-Pentane

To calculate the heat capacity values from enthalpy values derived from the work of Sage and Lacey (61), the following equation is applied:

TABLE V

Enthalpy Values for n-Pentane, Btu/lb

Pressure, psia	Data Sources	Temperature, °F 100	160	220	280	340	400
400	I	-	-	219.5	258.6	306.4	419.3
	II	-	-	217.3	258.5	305.6	419.3
	III	144.5	180.6	218.6	259.6	306.6	418.1
	IV	145.1	182.0	222.0	265.0	310.8	-
500	I	-	-	219.6	258.7	304.5	400.6
	II	-	-	217.1	258.2	304.6	401.2
	III	144.7	180.8	218.6	259.4	305.2	402.0
	IV	145.5	182.1	221.6	264.0	309.1	-
800	I	-	-	220.4	259.0	302.4	355.6
	II	-	-	216.6	257.3	302.4	353.0
	III	145.4	181.4	218.9	259.1	303.1	351.2
	IV	146.5	182.5	221.0	262.1	305.8	-
1000	I	-	-	220.5	259.6	302.0	350.8
	II	-	-	216.3	256.6	301.4	348.9
	III	145.9	181.8	219.2	259.0	302.2	347.7
	IV	147.1	182.9	221.0	261.5	304.5	-

I Curl and Pitzer (16)

II Lenoir, Robinson, and Hipkin (32)

III Sage and Lacey (61)

IV Yen and Alexander (77)

$$C_p = C_p^o - \frac{\Delta H(t_b,P) - \Delta H(t_a,P)}{t_b - t_a} \qquad (24)$$

In the above equation C_p is the heat capacity of n-pentane at the average temperature of t_a and t_b and the pressure P, and C_p^o the corresponding ideal gas heat capacity. The equation presented by Yen and Alexander (77) for the reduced enthalpy departure, i.e., Equation 21, has been differentiated with respect to reduced temperature to generate a generalized equation of heat capacity departure for compressed liquids in the z_c=0.27 group. The equation has the form

$$\begin{aligned} \tilde{C}_p^o - \tilde{C}_p = & -14.56975 \\ & -15.625448\ (T_R - 0.79749) \\ & -0.1642482\ (P_R - 4.664) \\ & + \frac{4.463472}{T_R} \ln(P_R) \\ & + \frac{9.051662}{T_R} \ln(P_R)\ \ln(T_R) \end{aligned} \qquad (25)$$

The heat capacity values of n-pentane at the desired reduced temperature T_R and reduced pressure P_R is calculated as

$$C_p = C_p^o - \frac{(\tilde{C}_p^o - \tilde{C}_p)}{M} \qquad (26)$$

The generalized graphs prepared by Edmister (19) for the heat capacity departure functions $(\tilde{C}_p - \tilde{C}_p^o)^{(o)}$ and $(\tilde{C}_p - \tilde{C}_p^o)^{(1)}$ were derived from the values of $(\frac{\tilde{H}^o - \tilde{H}}{RT_c})^{(o)}$ and $(\frac{\tilde{H}^o - \tilde{H}}{RT_c})^{(1)}$ which were presented by Curl and Pitzer (16). Both the reduced enthalpy departure tables presented by Curl and Pitzer(16)

and the heat capacity departure graphs presented by Edmister (19) are not applicable for reduced temperatures lower than 0.8. For n-pentane, T_R=0.8 at 216°F. The differentiation of the enthalpy values calculated from the tables of Pitzer et al. (16) have generated heat capacity values in agreement with those calculated from Edmister's graphs for the region of this study. To calculate the isobaric heat capacity values using the graphs prepared by Edmister(19), the values of $(\tilde{C}_p-\tilde{C}_p^o)^{(0)}$ and $(\tilde{C}_p-\tilde{C}_p^o)^{(1)}$ were read from the corresponding graphs for a number of reduced temperatures at a fixed reduced pressure. Similar procedures were followed at other reduced pressures. The values so obtained produced plots of $(\tilde{C}_p-\tilde{C}_p^o)^{(0)}$ versus T_R and $(\tilde{C}_p-\tilde{C}_p^o)^{(1)}$ versus T_R for each reduced pressure. Then values of $(\tilde{C}_p-\tilde{C}_p^o)^{(0)}$ and $(\tilde{C}_p-\tilde{C}_p^o)^{(1)}$ were obtained by interpolation at 20°F intervals. The heat capacity departure is calculated through Equation 5, and the isobaric heat capacity is calculated as

$$C_p = C_p^o + \frac{(\tilde{C}_p-\tilde{C}_p^o)}{M} \qquad (27)$$

In the above calculations, the ideal gas heat capacity values are obtained from API Technical Data Book (2).

It has been found that the enthalpy values presented by Lenoir et al. (32) do not seem to be smooth enough to warrant calculation of isobaric heat capacity values by numerical differentiation of the enthalpy values at two adjacent

temperatures. Therefore, polynomials in temperature have been used to fit the enthalpy values through least squares method. The polynomials for 400, 500, and 1,000 psia are 5th order while that for 800 psia is 4th order. For each isobar, at least ten data points have been used to develop the least squares polynomial. The heat capacity values are then obtained by differentiation of the polynomials with respect to temperature.

The calculated heat capacity values are plotted in Figures through 17 to compare with the experimental values obtained in this study. The values derived from the work of Sage and Lacey (61), from the enthalpy data of Lenoir et al. (32), and from the graphs of Edmister are presented in Figures 8 through 14, while those derived from the calculated enthalpy of Brydon et al. (9) and from the equation of Yen and Alexander (77) are presented in Figures 15 through 17.

As shown in Figures 8 through 14, the maximum differences between the values calculated from Edmister's graphs and those derived from the work of Sage and Lacey amount to 5%. This discrepancy is more obvious for the low pressure region. In the region of this study, the differences between the heat capacity values derived from the work of Sage and Lacey (61) and those calculated from the enthalpy data of Lenoir et al. (32) are small. It can be seen that at low temperature region those calculated from the work of Sage and Lacey (61) have

larger values, while at high temperature region larger values are observed for those derived from the work of Lenoir et al. (32). It is expected that as the temperature approaches the critical point, the differences would be more significant. The experimental values obtained in this study fall between the values calculated by these methods for the low temperature region while at high temperature region the experimental values are smaller than the calculated values. The experimental values agree with the values calculated from the work of Sage and Lacey (61) within 1% except at the low pressure and high temperature region where differences as high as 3% are observed.

Both the values calculated from the equation of Yen and Alexander (77) and the values calculated from the enthalpy values of Brydon et al. (9) do not show good agreement with the experimental values. It is interesting to know that these calculated values do not agree with each other although that Yen and Alexander (77) used the enthalpy values presented by Brydon et al. (9) to develop the equation of the reduced enthalpy departure. It can be seen from Figures 15 through 17 that the disagreements become more serious as the temperature approaches the critical point.

The generalized correlation presented by Yuan and Stiel (83) for the prediction of the heat capacity of saturated non-polar liquids has been used to calculate the heat capacity of saturated liquid n-pentane. Their method has been tested

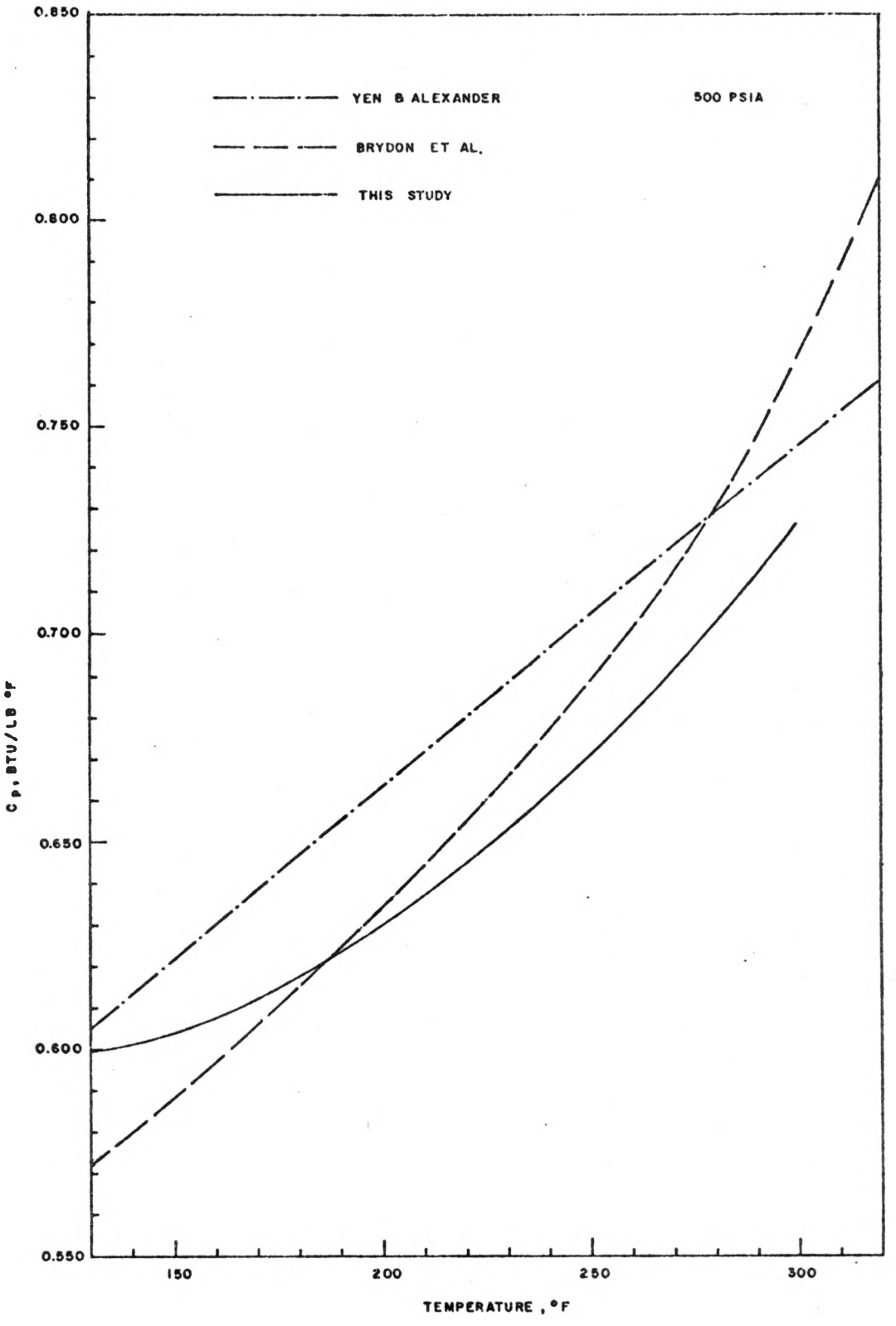

Figure 15. Comparison of experimental results for n-pentane with calculated values

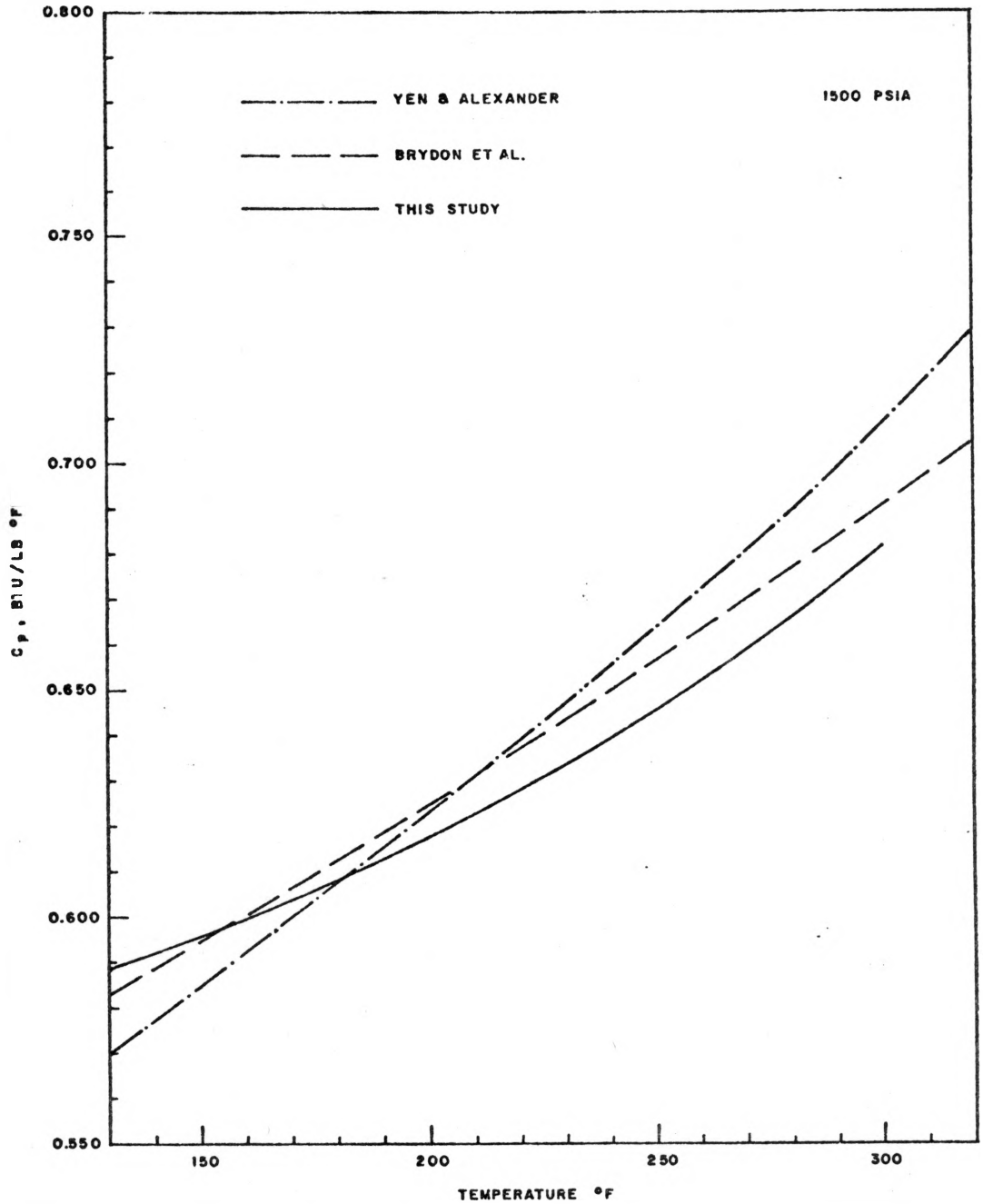

Figure 16. Comparison of experimental results for n-pentane with calculated values

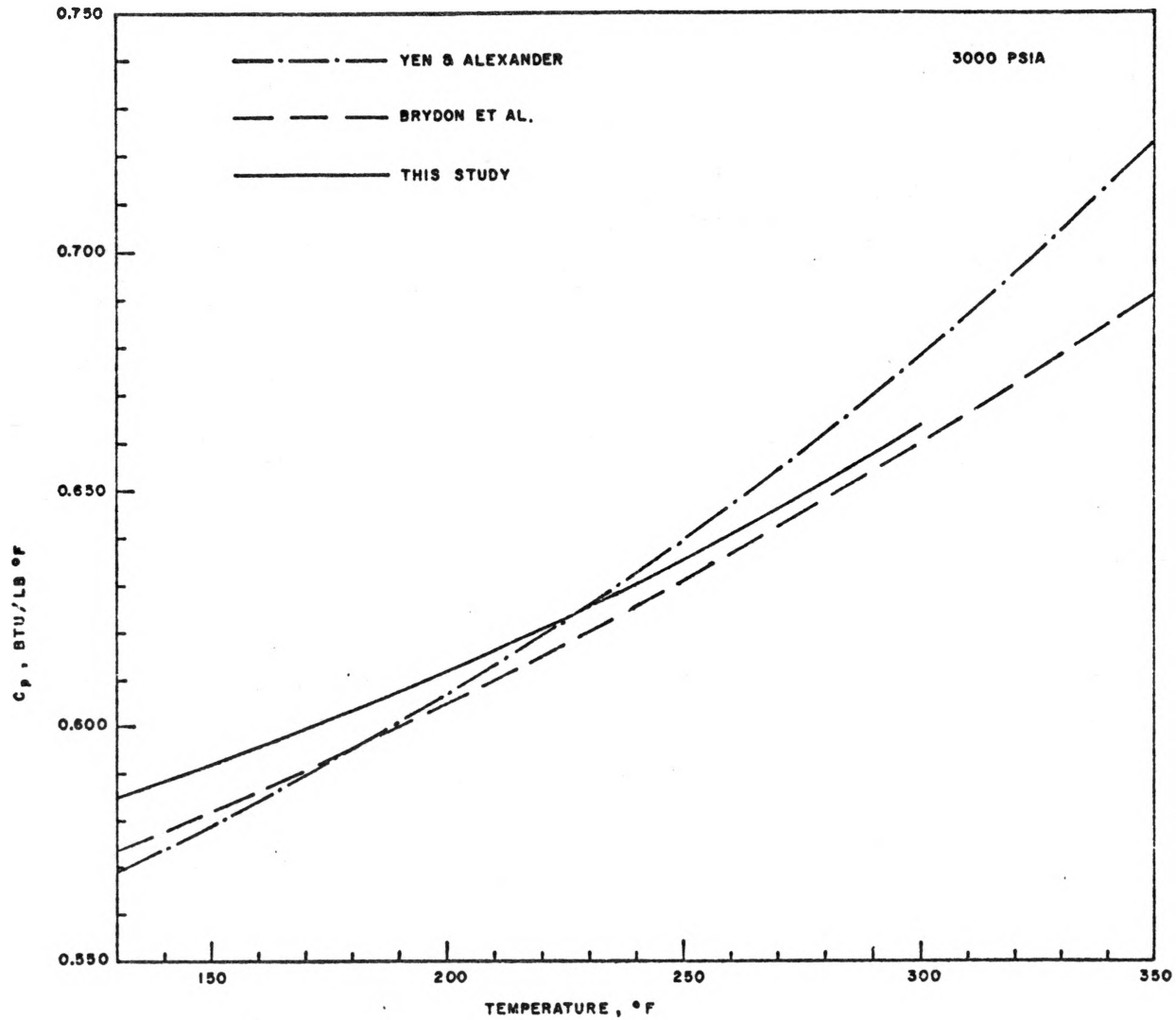

Figure 17. Comparison of experimental results for n-pentane with calculated values

with 21 non-polar liquids over the reduced temperature range of T_R=0.4 to T_R=0.96 and found to be quite reliable (83). The calculated heat capacity values of saturated liquid n-pentane are plotted against pressure as shown in Figure 18. The smoothed isotherms of experimental heat capacity values and the values calculated from the works of Sage and Lacey (61) and of Edmister (19) are also plotted in Figure 18. The experimental isotherms are extrapolated from 400 psia to the saturation pressures at respective temperatures and intersect the saturation line at almost the exact heat capacity values for the saturated liquid at all temperatures while large deviations would happen for the calculated heat capacity values. The consistency of the experimentally determined heat capacity values and the heat capacities for saturated liquid helps to substantiate the reliability of the experimental data obtained in this study.

The disagreement between the heat capacity values calculated through Edmister's generalized graphs and the experimental data obtained in this study has prompted the comparisons of experimental heat capacity values for other substances. Therefore, experimental heat capacity values of methane (24), nitrogen (39), and propane (80) were obtained and the heat capacity departures are calculated at reduced pressures of 0.817, 1.022, and 2.043 and reduced temperatures of 0.80, 0.85, and 0.90. The results are plotted in Figures

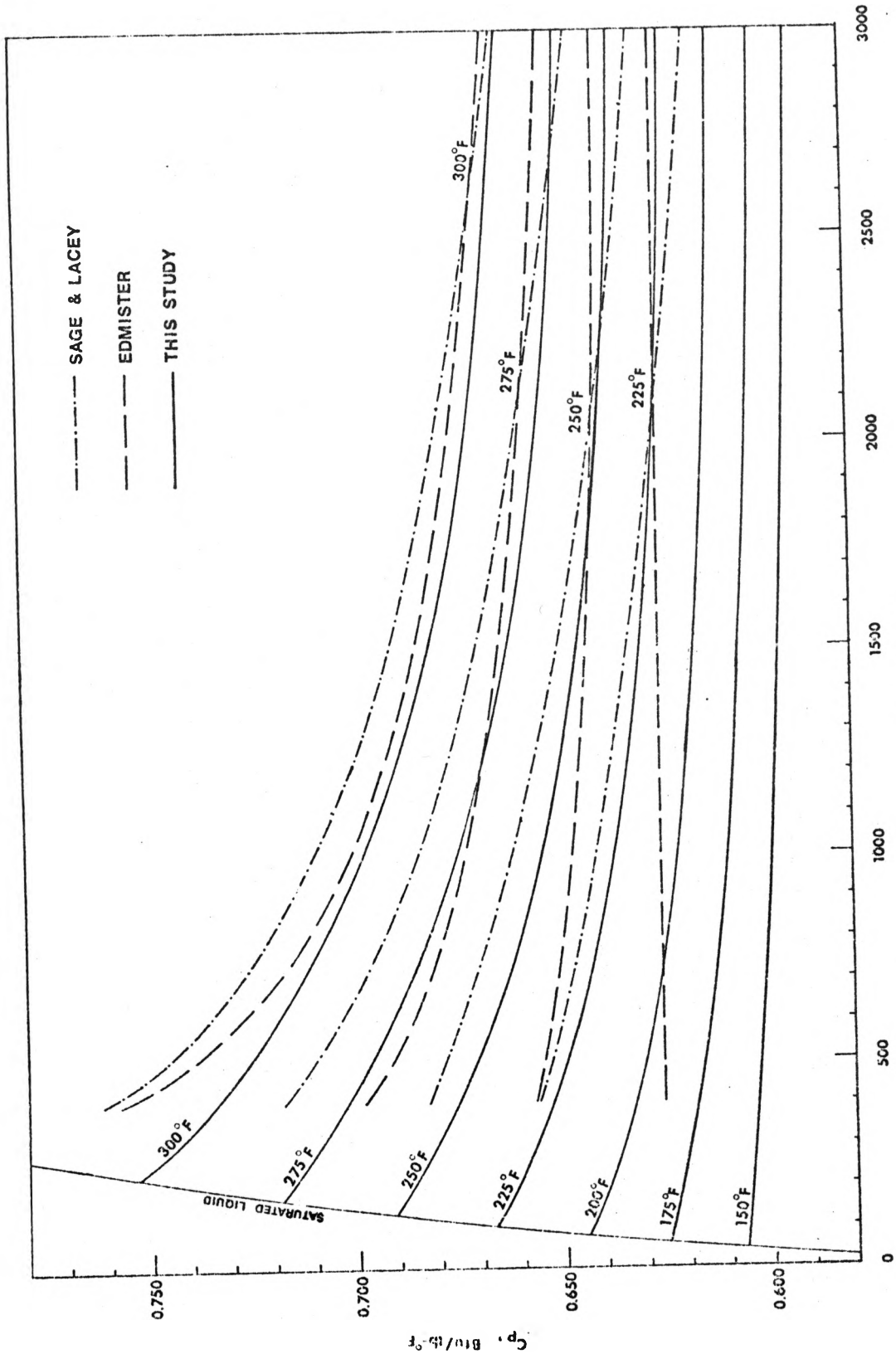

Figure 18. Heat capacity of n-pentane

19 through 21 with the values for n-pentane also included. It can be seen that the behavior of n-pentane agrees with those for other non-polar fluids, and it is obvious that the graphs presented by Edmister (19) need to be refined so that more reliable predicted values can be obtained. Based on these four substances, suggested lines are drawn in Figures 19 through 21.

It is obvious that almost all calculated heat capacity values are higher than the experimentally determined values as the temperature approaches the critical point. This could be because for this region the volumetric behavior of the liquid is more sensitive to temperature and the calculated values become less reliable. Although the experimental enthalpy data of Lenoir et al. (32) are the quantities which are most closely related to the heat capacity values, the possible lack of precision or errors in their enthalpy values have reduced the reliability of the derived heat capacity values. A plot showing the point values of heat capacity obtained by numerical differentiation of the enthalpy values of Lenoir et al. (32), the smoothed heat capacity values obtained by differentiation of the least squares polynomial for the enthalpy values of Lenoir et al. (32), and the experimental results obtained in this study is presented in Figure 22 for the pressure of 1,000 psia.

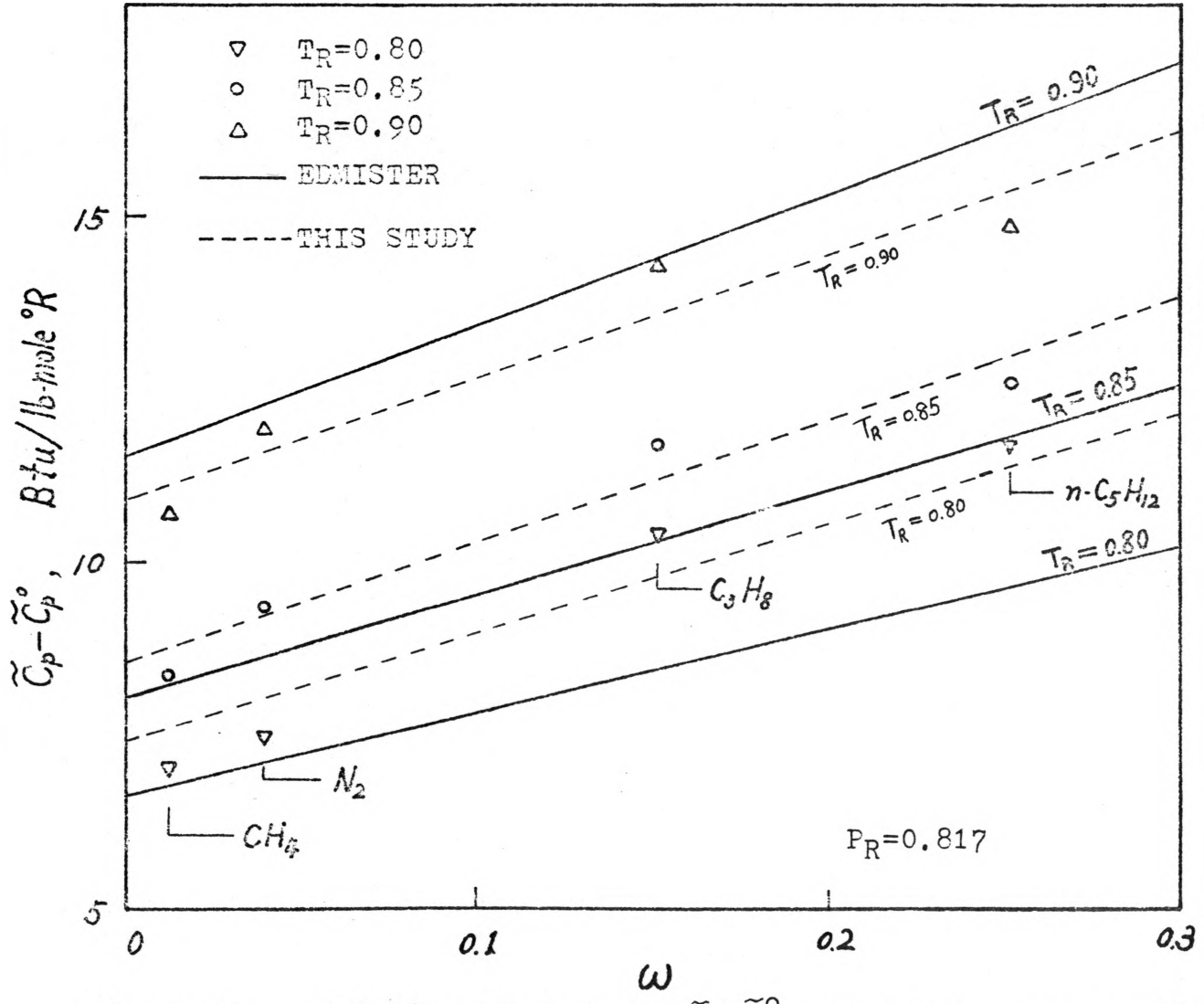

Figure 19. Relationship between $\tilde{C}_p$-$\tilde{C}_p^o$ and ω for non-polar liquids

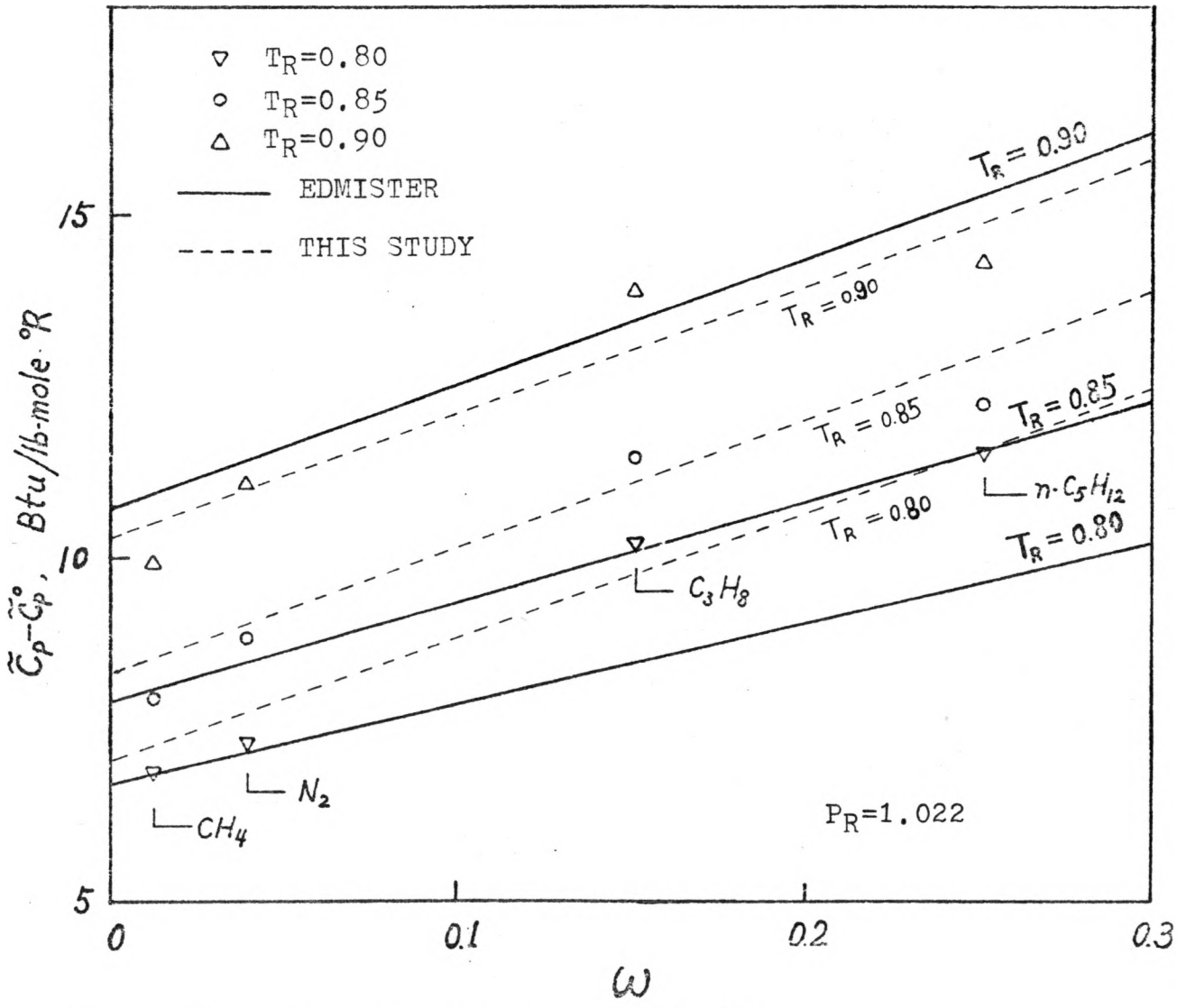

Figure 20. Relationship between $\tilde{C}_p - \tilde{C}_p^\circ$ and ω for non-polar liquids

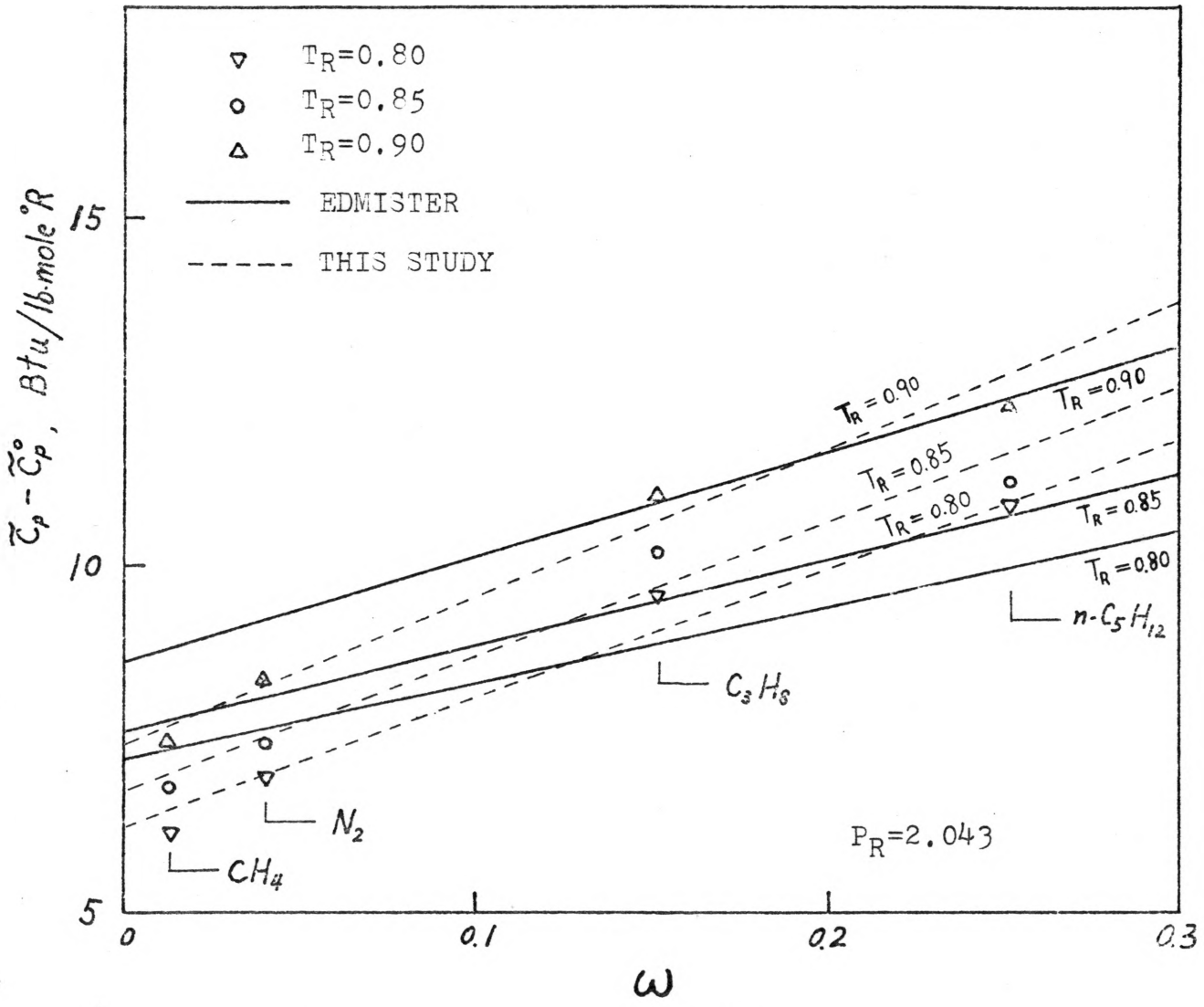

Figure 21. Relationship between $\tilde{C}_p$-$\tilde{C}_p^o$ and ω for non-polar liquids

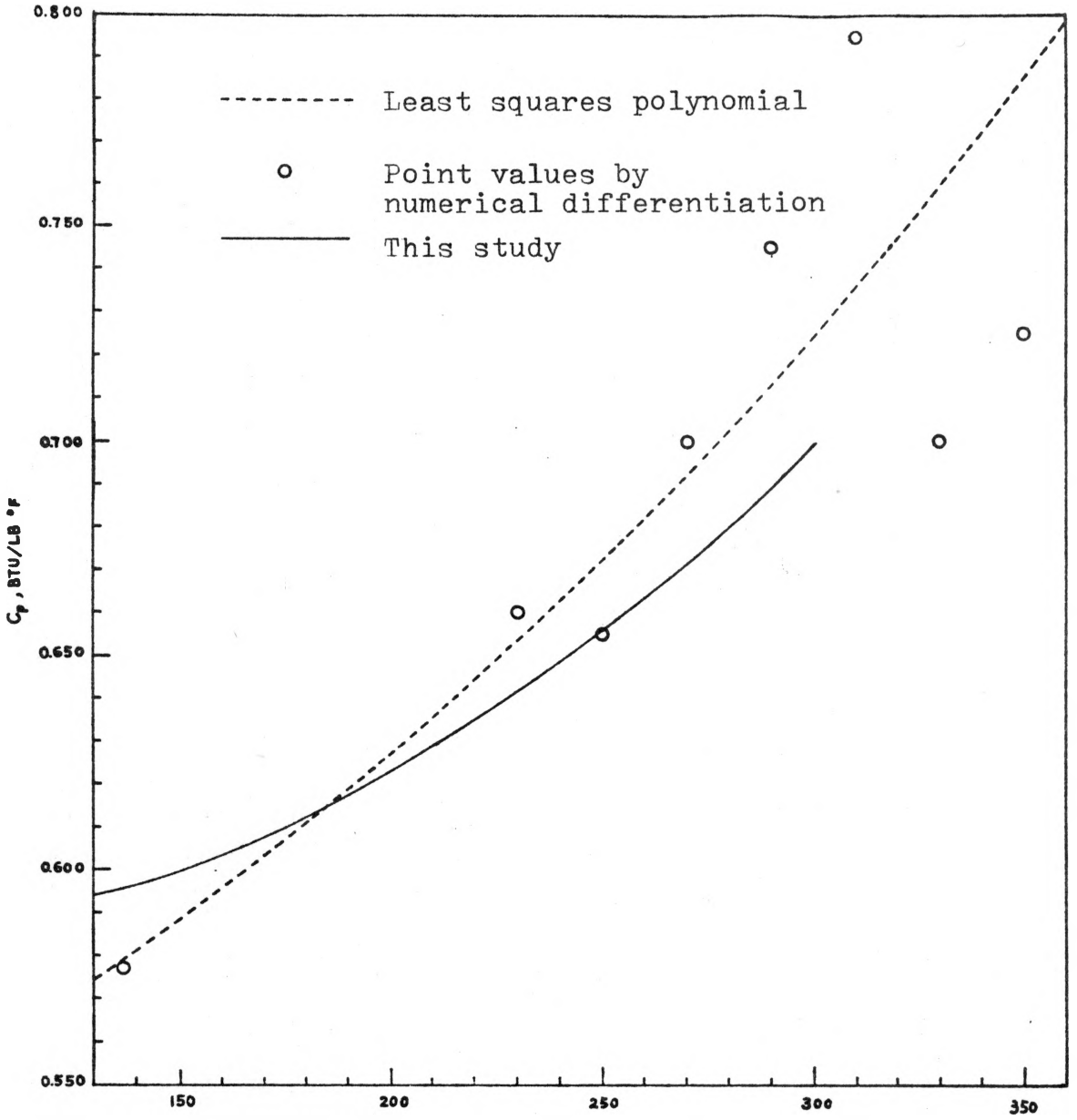

Figure 22. Comparison of experimental results for n-pentane with values calculated from the enthalpy values of Lenoir et al. at 1000 psia

CHAPTER VIII

DISCUSSION AND CONCLUSIONS

The isobaric heat capacities of n-pentane in the liquid region have been experimentally determined using a flow calorimeter system. The use of a closed-loop system has limited the accuracy of the determination of the mass flow rate. It can be seen that over one-half of the total error in the heat capacity value are due to the error in the calculation of the mass flow rate which is the product of the volumetric flow rate and the density value. However, the advantages of minimum test fluid consumption, smaller space requirement, and comparably easier attainability and control of steady state have offset this disadvantage. As indicated in Chapter IV, the "O" ring seal in the stuffing box of the turbine pump has caused difficulties in the experiments. It is recommended that, for future work, a sealless and leak-proof pump, such as a magnet-driven pump, be used in place of the turbine pump to eliminate the imperfection of the experimental system.

Comparisons have shown that the experimental results agree most closely with the values derived from experimental density data, and are believed to be more reliable than any of the calculated values. The following conclusions can be drawn from this study:

1) If accurate density data are available, reliable enthalpy values and therefore good heat capacity values can be calculated using rigorous thermodynamic relations. Since a double differentiation is involved in this method, loss of accuracy should be expected. The greater difference (maximum difference of 3%) existing in the low pressure and high temperature region between the experimental heat capacity values and the values derived from the experimental P-V-T data presented by Sage and Lacey (61) may be due to the error in the derivatives of volumetric data. The volumetric behavior of liquid n-pentane is more sensitive to temperature in this region and consequently larger error may be introduced by a differentiation process. More experimental heat capacity data for n-pentane at higher temperatures are required to help ascertain the reliability of the calculated heat capacity values in this region.

2) The large difference found between the values calculated using Edmister's generalized graphs (19) and the experimental data is most likely due to the fact that any generalized correlation is inherently subject to error and that differentiation of the generalized equation with respect to any of its parameters will inevitably increase the order of magnitude of the error in the derived correlation. The fact that the heat capacity data determined in this study are consistent with experimental data for the heat capacity of the saturated

liquids not only has substantiated the reliability of the experimental apparatus and results, but also has revealed the necessity of a more reliable generalized method for the prediction of heat capacity departure of non-polar liquid.

3) The equation presented by Yen and Alexander (77) for the reduced enthalpy departure of compressed liquid should not be differentiated to produce equations for heat capacity departure. Although fairly good agreement has been found for the enthalpy values (77), large errors may result for the heat capacity values.

4) The experimental results have shown that at pressures greater than 2,000psia (P_R=4.08) the effect of the pressure upon the heat capacity of n-pentane liquid becomes less significant. For temperatures below 200°F (T_R=0.78) the heat capacity isotherms as shown in Figure 15 are almost independent of pressure for pressures greater than 2,000 psia. At 300°F, the highest temperature investigated, less than 1.5% change of C_p values are observed while the pressure is increased from 2,000 psia to 3,000 psia.

5) The accuracy of the heat capacity data obtained using a closed-loop flow calorimeter system can be considerably enhanced when density-independent mass flowmeter becomes available and is applied.

LITERATURE CITED

1. Altunin, V. V., and D. O. Kuznetsov, Teploenergetika, 16(8), 82 (1969).

2. American Petroleum Institute, "Technical Data Book-Petroleum Refining", 2nd ed., Chapter 7, Washington, D.C. (1971).

3. Barieau, R. E., U.S. Bur. Mines Inform. Circ., 8245 (1965).

4. Beattie, J. A., S. W. Levine, and D. R. Douslin, J. Am. chem. Soc., 74, 4778 (1952).

5. Blackett, P. M. S., P. S. H. Henry, and E. K. Rideal, Proc. Roy. Soc. (London), A126, 319 (1930).

6. Bondi, A., Ind. Eng. Chem. Fundamentals, 5, 443 (1966).

7. Brinkworth, J. H., Proc. Roy. Soc. (London), A107, 510 (1925).

8. Brinkworth, J. H., Proc. Roy. Soc. (London), A111, 124 (1926).

9. Brydon, J. W., N. Walen, and L. N. Canjar, Chem. Eng. Prog. Symp. Ser., 49 (7), 151 (1953).

10. Callendar, H. L., World Power, 3, 302 (1925).

11. Callendar, H. L., and H. T. Barnes, Phil. Trans., 199A, 55 (1902).

12. Clark, R. G., and C. McKinley, in:"Advances in Cryogenis Engineering", Vol. 14, Plenum Press, New York (1969).

13. Clark, A. L., and L. Katz, Can. J. Res., 18A, 23 (1940); 21A, 1 (1943).

14. Cornish, R. E., and E. D. Eastman, J. Am. Chem. Soc., 50, 627 (1928).

15. Crawford, A., Expts. and Obs. on Animal Heat, pp. 167, seq., (1788).

16. Curl, R. F. Jr., and K. S. Pitzer, Ind. Eng. Chem., 50, 265 (1958).

17. DeNevers, N., and J. J. Martin, A. I. Ch. E. J., 6, 43 (1960).

18. Din, F., ed., "Thermodynamic Functions of Gases", Vols 1-3, Butterworths, London (1961).

19. Edmister, W. C., Hydrocarbon Processing, 46 (5), 187 (1967).

20. Faulkner, R. C. Jr., Ph.D. thesis, Univ. of Michigan, (1959).

21. Ginnings, D. C., "Introduction", in "Experimental Thermodynamics, Vol. 1", J. P. McCullough, and D. W. Scott, Plenum Press, New York, ed., (1968).

22. Halm, R. L., and L. I. Stiel, A. I. Ch. E. J., 13, 351 (1967).

23. Hubbard, J. C., and A. H. Hodge, J. Chem. Phys., 5, 978 (1937).

24. Jones, M. L., Jr., D. T. Mage, R. C. Faulkner, Jr., and D. L. Katz, Chem. Eng. Prog. Symp. Ser., 59 (44), 52 (1963).

25. Joule, J. P., and W. Thomson, Phil. Mag., Ser. 4, 4, 481 (1852).

26. Keyes, F. G., and S. C. Collins, Proc. Natl. Acad. Sci. (U.S.), 18, 328 (1932).

27. King, R. C., and J. H. Potter, J. Eng. Ind., 84, 180 (1962).

28. Kistiakowsky, G. B., and W. W. Rice, J. Chem. Phys., 7, 281 (1931).

29. Koehler, W. F., J. Chem. Phys., 18, 465 (1950).

30. Krase, N. W., and B. H. Mackey, J. Am. Chem. Soc., 52, 108 (1930).

31. Krase, N. W., and B. H. Mackey, J. Am. Chem. Soc., 52, 51111 (1930).

32. Lenoir, J. M., D. R. Robinson, and H. G. Hipkin, J. Chem. Eng. Data, 15, 23 (1970).

33. Lenoir, J. M., K. E. Hayworth, and H. G. Hipkin, J. Chem. Eng. Data, 15, 474 (1970).

34. Lenoir, J. M., G. K. Kuravila, and H. G. Hipkin, J. Chem. Eng. Data, 16, 271 (1971).

35. Lenoir, J. M., C. J. Robert, and H. G. Hipkin, J. Chem. Eng. Data, 16, 401 (1971).

36. Li, K., and L. N. Canjar, Chem. Eng. Prog. Symp. Ser., 49 (7), 147 (1953).

37. Lydersen, A. L., R. A. Greenkorn, and O. A. Hougen, Univ. Wis. Eng. Exp. Sta. Rept. 4 (1955).

38. Mackey, B. H., and N. W. Krase, Ind. Eng. Chem., 22, 1060 (1930).

39. Mage, D. T., M. L. Jones, Jr., D. L. Katz, and J. R. Roebuck, Chem. Eng. Prof. Symp. Ser., 59 (44), 61 (1963).

40. Masi, J. F., Trans. A. S. M. E. 76, 1067 (1954).

41. Mather, A. E., Ph.D. thesis, Univ. of Michigan, (1967).

42. McCullough, J. P., D. W. Scott, H. L. Finke, W. N. Hubbard, M. E. Gross, C. Katz, R. E. Pennington, J. F. Messerly, and G. Waddington, J. Am. Chem. Soc., 75, 1818 (1953).

43. Michels, A., and J. C. Strijland, Physica, 16, 813 (1950).

44. Osborne, N. S., H. F. Stimson, and T. S. Sligh, Jr., U.S. Natl. Bur. Stds. Sci. Papers, 20, 119 (1925).

45. Osborne, N. S., H. F. Stimson, T. S. Sligh, Jr., and C. S. Cragoe, Ibid., 20, 65 (1925).

46. Osborne, N. S., H. F. Stimson, and D. C. Ginnings, J. Res. Natl. Bur. Stads., 23, 197 (1939).

47. Partington, J. R., and A. B. Howe, Proc, Roy. Soc. (London), A109, 286 (1925).

48. Partington, J. R., and W. G. Shilling, "The Specific Heats of Gases", D. Van Nostrand Co., New York (1924).

49. Pattee, E. C., and G. G. Brown, Ind. Eng. Chem., 26, 511 (1934).

50. Pitzer, K. S., J. Am. Chem. Soc., 63, 2413 (1941).

51. Pitzer, K. S., Ind. Eng. Chem., 36, 829 (1944).

52. Pitzer, K. S., and J. E. Kilpatrick, Chem. Rev., 39, 435 (1946).

53. Pitzer, K. S., D. Z. Lippmann, R. F. Curl, Jr., C. M. Huggins, and D. E. Peteren, J. Am. Chem. Soc., 77, 3433 (1955).

54. Reid, R. C., and J. R. Valbert, Ind. Eng. Chem. Fundamentals, 1, 292 (1962).

55. Reid, R. C., and T. K. Sherwood, "The Properties of Gases and Liquids", McGraw-Hill, New York (1966).

56. Rivkin, S. L., and V. M. Gukov, Teploenergetika, 15 (10), 72 (1968).

57. Roebuck, J. R., Proc, Am. Acad. Arts Sci., 60, 537 (1925).

58. Rose-Innes, J., and S. Young, Phil. Mag., 47, 353 (1899).

59. Rossini, F. D., et al, "Selected Values of Physical and Thermodynamic Properties of Hydrocarbons and Related Compounds", Carnegie Press, Pittsburgh, pa. (1953).

60. Sage, B. H., H. S. Backus, and T. Vermeulen, Ind. Eng. Chem., 28, 489 (1936).

61. Sage, B. H., and W. N. Lacey, Ind. Eng. Chem., 34, 730 (1942).

62. Sage, B. H., W. N. Lacey, and J. G. Schaafsma, Ind. Eng. Chem., 27, 48 (1935).

63. Scheindlin, A. E., V. V. Sychev, M. M. Khilal, and N. I. Gorbunova, Teploenergetika, 10 (9), 76 (1963).

64. Schrock, V. E., N. A. C. A., Technical Note 2838, December (1952).

65. Sherratt, G. G., and E. Griffiths, Proc. Roy. Soc. (London), A147, 292 (1934).

66. Sherratt, G. G., and E. Griffiths, Proc. Roy. Soc. (London), A156, 504 (1936).

67. Sirota, A. M., and B. K. Mal'tsev, Teploenergetika, 6 (9), 7 (1959).

68. Sirota, A. M., and A. Ya. Grishkov, Teploenergetika, 13 (8), 61 (1966).

69. Sirota, A. M., and Z. Kh. Shrago, Teploenergetika, 15 (3), 24 (1968).

70. Sirota, A. M., and A. Kh. Shrago, Teploenergetika, 15 (8), 86 (1968).

71. Sirota, A. M., A. Ya. Grishkov, and A. G. Tomishko, Teploenergetika, 17 (9), 60 (1970).

72. Timmermans, J., Sci. Proc. Roy. Dublin Soc., 13, 310 (1912).

73. Voronel', A. V., and P. G. Strelkov, Cryogenics, 2, 91 (1961).

74. Waddington, G., S. S. Todd, and G. M. Huffman, J. Am. Chem. Soc., 69, 22 (1947).

75. Weiss, A. H., and J. Joffe, Ind. Eng. Chem., 49, 120 (1957).

76. Wiener, L. D., paper presented at 58th National A. I. Ch. E. Meeting, Dallas (1966).

77. Yen, L. C., and R. E. Alexander, A. I. Ch. E. J., 11, 334 (1965).

78. Yesavage, V. F., A. E. Mather, D. L. Katz, and J. E. Powers, Ind. Eng. Chem., 59 (11), 35 (1967).

79. Yesavage, V. F., D. L. Katz, and J. E. Powers, J. Chem. Eng. Data, 14, 137 (1969).

80. Yesavage, V. F., D. L. Katz, and J. E. Powers, J. Chem. Eng. Data, 14, 197 (1969).

81. Young, S. Sci. Proc. Roy. Dublin Soc., 12, 374 (1910).

82. Yuan, T. F., M.S. thesis, Syracuse University (1968).

83. Yuan, T. F., and L. I. Stiel, Ind. Eng. Chem. Fundamentals, 9, 393 (1970).

NOMENCLATURE

C = Heat capacity, Btu/lb^{o}F

C_p = Heat capacity at constant pressure, Btu/lb^{o}F

C_p^o = Ideal-gas heat capacity at constant pressure, Btu/lb^{o}F

$\tilde{C}_p$ = Heat capacity at constant pressure, Btu/lb-mole^{o}F

$\tilde{C}_p^o$ = Ideal gas heat capacity at constant pressure, Btu/lb-mole^{o}F

$\tilde{C}_\sigma$ = Heat capacity of saturated liquid, Btu/lb-mole^{o}F

$\Delta\tilde{C}_\sigma$ = $\tilde{C}_\sigma - \tilde{C}_p^o$, Btu/lb-mole^{o}F

E = Voltage drop, volts

f = Frequency, cycles/sec

$\tilde{H}$ = Enthalpy, Btu/lb-mole

$\tilde{H}^o$ = Enthalpy at ideal-gas state, Btu/lb-mole

H = Enthalpy, Btu/lb

H^o = Enthalpy at ideal-gas state, Btu/lb

ΔH = $H^o - H$, Btu/lb

I = Current, amperes

m = Mass, lb

$\dot{m}$ = Mass flow rate, lb/sec

M = Molecular weight, lb/lb-mole

P = Pressure, psia

P_c = Critical pressure, psia

P_R = Reduced pressure, P/P_c

Q = Energy, Btu

R = Gas constant, 1.987 Btu/lb-mole^{o}R

r_v = Residual volume, ft^3/lb

t = Temperature, ^oF

T = Absolute temperature, ^oR

T_c = Critical temperature, ^oR

T_R = Reduced temperature, T/T_c

ΔT = Temperature difference, ^oF

v = Specific volume, ft^3/lb

V = Volumetric flow rate, gal/min

W = Power, Btu/sec

x = Parameter, defined in Equation 10

z = Compressibility factor

z_c = Critical compressibility factor

z_T = Derivative compressibility factor

Greek Letters

α, β, and γ = Coefficients in Equation 14

μ_o, μ, η_o, η, ρ_o, and ρ = Coefficients in Equation 2

ρ = Density, lb/ft^3

ω = Acentric factor, defined in Equation 4

Subscripts and Superscripts

1 = Calorimeter inlet condition

2 = Calorimeter outlet condition

(0) = Simple fluid function

(1) = Normal fluid correction term

(2) = Polar fluid correction term

(3), (4), (5) = Coefficients for higher order terms for series expansions in ω and x

APPENDIX A

Calibration Data

TABLE A-1

Calibration Data of Main Thermocouples

Temperature	Thermoelectric Voltage in Millivolts *				
°C	IPTS Value	No. 1	No. 2	No. 3	No. 4
50.85	2.0775	2.0773	2.0769	2.0770	2.0771
60.23	2.4771	2.4787	2.4783	2.4785	2.4786
69.88	2.9031	2.9050	2.9045	2.9047	2.9047
80.05	3.3592	3.3610	3.3606	3.3607	3.3608
89.95	3.8107	3.8124	3.8120	3.8122	3.8123

* Reference junctions at 0°C.

TABLE A-2

Calibration Data of Thermocouples for

Measuring Flowmeter Temperatures

Reference Junctions at 0°C

Temperature	Thermoelectric Voltage in Millivolts		
°C	IPTS Value	Thermopile #1	Thermopile #2
50.30	2.0479	2.0498	2.0495
59.54	2.4672	2.4690	2.4685
70.25	2.9192	2.9210	2.9206
80.14	3.3633	3.3649	3.3644
90.35	3.8291	3.8309	3.8305

TABLE A-3

Calibration Data of Flowmeter

Run No.	f cycles/sec	V GPM	V_{calc} GPM
1	1811	2.1000	2.1013
2	1672	1.9390	1.9400
3	1404	1.6290	1.6291
4	1075	1.2480	1.2473
5	953.6	1.1070	1.1064
6	789.9	0.9182	0.9165
7	646.8	0.7510	0.7504
8	487.9	0.5652	0.5661
9	348.3	0.4021	0.4041
10	341.6	0.3947	0.3963
11	221.6	0.2560	0.2571
12	164.1	0.1909	0.1904

$$V_{calc} = 0.001160316\ f$$

TABLE A-4

Calibration Data of Pressure Transducers

Excitation Voltage : 10.000 ± 0.005 VDC

Applied Pressure psia	Transducers' Outputs v, millivolts		Calculated Pressures P_{calc}, psia	
	#4318	#4319	#4318	#4319
500	3.283	4.665	501.8	499.3
1000	6.338	8.095	1000.2	1001.0
1500	9.391	11.510	1498.4	1500.5
2000	12.453	14.920	1998.0	1999.3
2500	15.525	18.340	2499.2	2499.5
3000	18.610	21.765	3002.5	3000.5

$(P_{calc})_{4318} = 163.158\ v - 33.855$

$(P_{calc})_{4319} = 146.266\ v - 183.023$

APPENDIX B

Derivation of Equation 12

and

Sample Calculation

(1) Derivation of Equation 13

The first law of thermodynamics, applied to a flow calorimeter with negligible heat leak and in which the changes of kinetic and potential energies of the fluid are negligible, is

$$H_{t_2,P_2} - H_{t_1,P_1} = \frac{-W}{\dot{m}} \qquad \text{(B-1)}$$

where H is the enthalpy per unit mass of the fluid at the indicated temperature and pressure, -W the rate of energy input, and $\dot{m}$ the mass flow rate. Subscripts 1 and 2 refer to the inlet and the outlet of the calorimeter respectively.

Equation B-1 can be rewritten as

$$H_{t_2,P_2} - H_{t_2,P_1} + H_{t_2,P_1} - H_{t_1,P_1} = \frac{-W}{\dot{m}} \qquad \text{(B-2)}$$

Rearranging and dividing through Equation B-2 by t_2-t_1, we have

$$\left(\frac{H_{t_2} - H_{t_1}}{t_2 - t_1}\right)_{P_1} = \frac{-W}{\dot{m}(t_2-t_1)} - \frac{(H_{P_2} - H_{P_1})_{t_2}}{t_2 - t_1} \qquad \text{(B-3)}$$

The left-hand side of Equation B-3 can be interpretted as the isobaric heat capacity of the fluid at the pressure P_1 and the average temperature of t_1 and t_2. The second term on the right-hand side of Equation B-3 can be expressed as

$$\frac{P_2 - P_1}{t_2 - t_1}\left(\frac{\partial H}{\partial P}\right)_{t_2}$$

where $\left(\frac{\partial H}{\partial P}\right)_{t_2}$ is evaluated at t_2 and the average pressure of

P_1 and P_2. The rate of energy input, -W, is the product of the voltage applied and the current through the main heater of the calorimeter. Therefore we obtain

$$C_p = \frac{E \cdot I}{m(t_2-t_1)} - \frac{P_2-P_1}{t_2-t_1} \left(\frac{\partial H}{\partial P}\right)_{t_2} \qquad \text{(B-4)}$$

Expressing the mass flow rate, $\dot{m}$, by the product of the volumetric flow rate and the density and introducing conversion factors, we have

$$C_p = \frac{0.948 \times 10^{-3} \times 7.481 \times 60 \text{ v}}{0.001160316 \text{ f}} \frac{E \cdot I}{t_2-t_1} - \frac{P_2-P_1}{t_2-t_1}\left(\frac{\partial H}{\partial P}\right)_{t_2}$$

$$= 366.727 \cdot \frac{E \cdot I \cdot v}{f(t_2-t_1)} - \frac{P_2-P_1}{t_2-t_1}\left(\frac{\partial H}{\partial P}\right)_{t_2} \qquad \text{(B-5)}$$

where v is the specific volume of the fluid and f the frequency of the flowmeter output signal.

(2) Sample Calculation

Consider a point at 1,500 psia:

P_1 = 1500 psia

P_2 = 1495 psia

t_1 = 206.85°F

t_2 = 217.81°F

E = 131.40 volts

I = 4.450 amperes

f = 904 cycles/sec

v = 0.02880 ft^3/lb (at 218.4°F and 1495 psia)*

$\frac{\partial H}{\partial P}$ = 0.0016 Btu/lb psi (at 217.8°F and 1498 psia)*

$$C_p = \frac{366.727 \times 131.40 \times 4.450 \times 0.02880}{904 \times (217.81-206.85)} + 0.5 \times 0.0016$$

= 0.6241 Btu/lb°F

* Both v and $\frac{\partial H}{\partial P}$ are obtained by interpolation of tabulated values presented by Sage and Lacey (61).

VITA

Ding-yu Peng was born on September 28, 1943, in Hopei, China. He received the degree of Bachelor of Science in Engineering in 1966 from National Taiwan University, Taiwan, Republic of China. He served in the Chinese Army as second lieutenant from July 4, 1966 to July 3, 1967. He came to the United States of America in September 1968 to study at Syracuse University, Syracuse, New York. He transferred to the University of Missouri at Columbia in September 1969. He is a member of Tau Beta Pi.

The undersigned, appointed by the Dean of the Graduate Faculty, have examined a thesis entitled

Heat Capacity of n-Pentane Liquid at Elevated Pressures

presented by Ding-yu Peng

a candidate for the degree of Doctor of Philosophy

and hereby certify that in their opinion it is worthy of acceptance.

L. I. Stiel 12/12/72

Leonard I. Stiel

Richard M. Angus

Richard M. Angus

R. C. Warder Jr.

Richard C. Warder

University Libraries
University of Missouri

Digitization Information Page

Local identifier	Peng1972

Source information

Format	Book
Content type	Text with images
Source ID	Department copy
Notes	

Capture information

Date captured	March 2023
Scanner manufacturer	Fujitsu
Scanner model	fi-7460
Scanning system software	ScandAll Pro v. 2.1.5 Premium
Optical resolution	600 dpi
Color settings	8 bit grayscale
File types	tiff
Notes	

Derivatives - Access copy

Compression	Tiff: LZW compression
Editing software	Adobe Photoshop
Resolution	600 dpi
Color	grayscale
File types	tiff
Notes	Images cropped, straightened, brightened